Networks of enzymatically oxidized membrane lipids support calcium-dependent coagulation factor binding to maintain hemostasis

Sarah N. Lauder,[1,2] Keith Allen-Redpath,[1,2*] David A. Slatter,[1,2*] Maceler Aldrovandi,[1,2] Anne O'Connor,[1,2] Daniel Farewell,[3] Charles L. Percy,[1,2] Jessica E. Molhoek,[4] Sirpa Rannikko,[5] Victoria J. Tyrrell,[1,2] Salvatore Ferla,[6] Ginger L. Milne,[7] Alastair W. Poole,[8] Christopher P. Thomas,[1,2,6] Samya Obaji,[1,2] Philip R. Taylor,[1,2] Simon A. Jones,[1,2] Phillip G. de Groot,[4] Rolf T. Urbanus,[4] Sohvi Hörkkö,[5] Stefan Uderhardt,[9] Jochen Ackermann,[9] P. Vince Jenkins,[10] Andrea Brancale,[6] Gerhard Krönke,[9] Peter W. Collins[1,2†] Valerie B. O'Donnell[1,2†]

[1]Systems Immunity Research Institute, Cardiff University, Heath Park, Cardiff, CF14 4XN, UK. [2]Institute of Infection & Immunity, Cardiff University, Heath Park, Cardiff, CF14 4XN, UK. [3]Division of Population Medicine, Cardiff University, Heath Park, Cardiff, CF14 4XN, UK. [4]Department of Clinical Chemistry and Haematology, University of Utrecht, University Medical Center Utrecht, Utrecht, 3584 CX, The Netherlands, [5]Department of Medical Microbiology and Immunology, Research Unit of Biomedicine, University of Oulu, P.O.B 5000, FIN-90220, Finland and Medical Research Center and Nordlab Oulu, University Hospital, Oulu, 90220, Finland. [6]Welsh School of Pharmacy and Pharmaceutical Sciences, Cardiff University, Heath Park, Cardiff, CF14 4XN, UK. [7]Division of Clinical Pharmacology Vanderbilt University Medical Center, Nashville, Tennessee, TN 37240, USA, [8]School of Physiology, Pharmacy and Neuroscience, Medical Sciences Building, University Walk, Bristol BS8 1TD, UK. [9]Department of Internal Medicine and Institute for Clinical Immunology, University Hospital Erlangen, Erlangen, Germany, [10]Institute of Molecular Medicine, St James's Hospital, Dublin, Ireland.

*These authors contributed jointly to the work.

[†]Corresponding author. Email: o-donnellvb@cardiff.ac.uk (V.B.O'D.); collinspw@cardiff.ac.uk (P.W.C.).

One-sentence summary: Activation of an enzymatically oxidized phospholipid network from blood cells contributes to a human thrombotic disorder.

Abstract

Blood coagulation functions as part of the innate immune system by preventing bacterial invasion and it is critical to stopping blood loss (hemostasis). Coagulation involves the external membrane surface of activated platelets and leukocytes. Using lipidomic, genetic, biochemical, and mathematical modeling approaches, we found that enzymatically oxidized phospholipids (eoxPLs) generated by the activity of leukocyte or platelet lipoxygenases (LOXs) were required for normal hemostasis and promoted coagulation factor activities in a Ca^{2+}- and phosphatidylserine (PS)-dependent manner. In wild-type mice, hydroxyeicosatetraenoic acid-phospholipids (HETE-PLs)

enhanced coagulation and restored normal hemostasis in clotting-deficient animals genetically lacking p12-LOX or 12/15-LOX activity. Murine platelets generated 22 eoxPL species, all of which were missing in the absence of p12-LOX. Humans with the thrombotic disorder antiphospholipid syndrome (APS) had statistically significantly increased HETE-PLs in platelets and leukocytes, as well as greater HETE-PL immunoreactivity, than healthy controls. HETE-PLs enhanced membrane binding of the serum protein β2GPI (β2-glycoprotein I), an event considered central to the autoimmune reactivity responsible for APS symptoms. Correlation network analysis of 47 platelet eoxPL species in platelets from APS and control subjects identified their enzymatic origin and revealed a complex network of regulation, with the abundance of 31 p12-LOX-derived eoxPL molecules substantially increased in APS. In summary, circulating blood cells generate networks of eoxPL molecules, including HETE-PLs, which change membrane properties to enhance blood coagulation and contribute to the excessive clotting and immunoreactivity of patients with APS.

Introduction

Blood clotting is an essential first step in innate immunity; it is required to prevent bacterial invasion and ensure effective cessation of blood flow (hemostasis) after injury. Excess clotting in the vasculature underlies vascular inflammatory conditions, including myocardial infarction, stroke, pulmonary embolism, and deep vein thrombosis, whereas impaired coagulation contributes to excessive blood loss during surgery and childbirth, a common cause of mortality during childbirth. Thus, better understanding of the molecular processes underlying coagulation and hemostasis could drive the development of effective new treatments and inform prevention strategies for several major human disorders.

Hemostasis depends on the coagulation cascade, a series of serine proteases and cofactors in plasma. The coagulation cascade is initiated by tissue factor (TF). For clotting to occur, amino-phospholipid

(aPL) externalization on the surface of activated platelets is required. At the platelet membrane, scramblase leads to the translocation of phosphatidylethanolamine (PE) and phosphatidylserine (PS), providing a negative charge to facilitate calcium binding and factor association (1,2). Externalization of aPLs alone is only part of the physiological coagulation process, because the rare disorder Scott Syndrome presents with an inability to externalize PS and PE, but only a relatively minor bleeding phenotype, unless the patients are experiencing a severe hemostatic challenge (3). This suggests that additional PLs are involved.

Activated platelets and leukocytes rapidly generate oxidized PEs and phosphatidylcholines (PCs) through the action of lipoxygenase (LOX) enzymes. LOX-generated phospholipids are termed hydroxyeicosatetraenoic acid-phospholipids (HETE-PLs), and these lipids are present at or within the plasma membrane (4-10). HETE-PL positional isomers (in which the oxidized moiety can be located at one of up to six different positions on the fatty acid side chain) are cell type–specific and LOX isoform–dependent: 5-HETE-PLs are generated by human neutrophils, 12-HETE-PLs by platelets, and 15-HETE-PLs by monocytes/eosinophils. In mice, leukocytes express a 12/15-LOX homolog, which generates mainly 12-HETE-PLs, but also small amounts of 15-HETE-PLs (7). We previously identified cyclooxygenase 1 (COX-1)–derived, enzymatically oxidized PLs (eoxPLs) that are generated by platelets that have either prostaglandin E_2 (PGE_2), prostaglandin D_2 (PGD_2), or dioxolane A3 (DXA_3) (11,12). Using global lipidomics mass spectrometry, we identified 103 eoxPL molecular species in thrombin-activated human platelets (13). These data indicated that eoxPL generation is a broader phenomenon than was previously thought. However, the enzymatic origin of most members of this large group remains unknown.

Antiphospholipid syndrome (APS) is an acquired prothrombotic disorder caused by a diverse family of circulating “antiphospholipid” antibodies. These can be directed against phospholipids, including

PE or cardiolipin, or against proteins, such as the PL-binding protein β2-glycoprotein I (β2GPI) or other PL-binding proteins. In APS, pathogenic antibodies contribute to thrombotic episodes or pregnancy complications (14-16). An interaction between β2GPI and negatively charged phospholipids on the surface of cells is thought to be required for disease development (14,16). The phospholipids that provide optimal binding of β2GPI to membranes are unknown. Given that eoxPLs are generated by isolated blood cells and platelets, contain electronegative hydroxyl groups on their fatty acids, and remain cell-associated after their formation, we explored their generation in APS (4-10).

Here, we used biochemical, genetic, clinical, mathematical, and lipidomic approaches to reveal the pro-coagulant mechanisms of endogenously generated LOX-derived eoxPLs from platelets and leukocytes in vitro and in vivo. We found that LOX-derived eoxPLs increased the binding of β2GPI to membranes. We performed correlation network analysis of the 47 most abundant eoxPL species in platelets from a human APS cohort, which revealed several levels of enzymatic regulation. We found that increased amounts of eoxPLs were generated by blood cells from APS patients and that these lipids enhanced immune recognition in disease. Overall, our studies support the idea that hemostasis requires the generation of multiple eoxPL species by platelets and leukocytes, and that their production is chronically increased in human venous thrombotic disease associated with APS.

Results

HETE-PL species stimulate coagulation

Coagulation requires multiple complexes of enzymes and their cofactors. These complexes ultimately generate thrombin (also known as factor IIa, FIIa), the complex of tissue factor (TF) and Factor VIIa (FVIIa), the complex known as intrinsic tenase of factor IXa (FIXa) and factor VIIIa (FVIIIa), and the complex known as prothrombinase of factor Xa (FXa) and factor Va (FVa).

Coagulation requires multiple enzyme/cofactor complexes that ultimately generate thrombin (factor IIa, FIIa). These are termed (i) TF/FVIIa (extrinsic tenase), (ii) FIXa/FVIIIa (intrinsic tenase) and (iii) FXa/FVa (prothrombinase), and takes place on phospholipid membranes (17-19).

To support this cascade, plasma membranes externalize aminophospholipids (aPLs), PS and PE (18-21). PS is required to support coagulation; whereas PE enhances PS-mediated coagulation (1,2,22). PS and PE bind coagulation factors II, VII, IX and X in a calcium-dependent manner, through the gamma-carboxylated glutamic acid (Gla) domains on the coagulation factors (18,23), whereas FVIII and FV bind PS and PE directly through their C domains (24,25)). To examine the effects of HETE-PLs on coagulation, we incorporated specific HETE-PLs into TF-containing liposomes and added the liposomes to plasma. We monitored coagulation by measuring the production of thrombin. Increasing concentrations of 5-,12-, or 15-HETE-PE (Fig. 1A) or 5-,12-, or 15-HETE-PC (Fig. 1B) enhanced coagulation in a concentration-dependent manner.

The accepted model of coagulation is that PS supports the formation of the prothrombinase and intrinsic tenase complexes, and PE enhances the effect of PS (2). PC is thought to have no role in supporting coagulation. To determine the pro-coagulant mechanisms of HETE-PLs, we monitored thrombin generation varying PS concentrations in the presence of PE (2,26) or HETE-PE or HETE-PC. In the absence of PS, PE supported low thrombin generation, which increased upon substitution with 15-HETE-PE (Fig. 1C, left graphs). Increasing PS led to dose-dependent increases in thrombin generation, which were similarly increased by HETE-PE (Fig. 1C, left graphs). In contrast, neither PC nor HETE-PC supported thrombin generation without PE and PS (Fig. 1C, right graphs). Increasing PS led to a dose-dependent increase in thrombin generation with HETE-PC having an enhancing effect (Fig 1C, right graphs). The enhancing effect of HETE-PC was greater at higher PS concentrations than that for HETE-PE. The data indicated a mechanism by which HETE-PLs

enhance PS-dependent coagulation, in a manner similar to, but more potent, than that of PE. The pro-coagulant action of HETE-PC is highlighted because PC was previously assumed not to support PS in coagulation reactions (2,26).

Thrombin generation in platelet poor plasma is also influenced by anticoagulant factors (27) Therefore, we repeated the thrombin generation experiments in a synthetic system using purified proteins (FII, FV, FVII, FVIII) at physiological concentrations without inhibitors of coagulation. We stimulated thrombin generation with TF-containing liposomes containing specific HETE-PE and HETE-PC species. 15- and 12- HETE-PE and 15-, 12-, and 5-HETE-PCs statistically significantly increased thrombin generation (Fig. 1, D).

Molecular modeling shows bending of HETE with localization of –OH at the membrane surface, and association with calcium molecules

A molecular dynamics simulation was performed to understand how the hydroxyl group of 12-HETE-PC would behave within the membrane. An available pre-equilibrated DOPC membrane with 128 molecules was modified to give a composition of 5% SAPS, 5 % SAPC, 30% SAPE, 55% DOPC, 5% 12-HETE-PC. This includes 3 molecules of PS and HETE-PC per leaflet. On one side, HETE-PCs were placed with HETEs buried in the membrane (in the yellow hydrophobic compartment), whereas on the other, they were placed in a bent-up configuration, with the –OH close to the polar membrane surface. During the 300-ns simulation, the system remained stable. During the 300-ns simulation, all of the HETE-PCs with HETEs pointing downwards changed conformation to place the -OH group at the charged surface of the membrane (blue), whereas those already in that configuration remained stable (Fig. 2, A to D, movie S1). In this upward-facing position, the –OH could establish a hydrogen bond with the nearby lipid phosphates, and in some cases, with the carboxylic acid group of a neighboring PS (Fig. 2D). The OH- also appeared to

interact with calcium ions (Fig. 2, B and C). As expected, calcium ions (red) strongly interacted with PS headgroups during the simulation (Fig. 2, C and D). As a result, both the HETE-OH and the PS carboxylic acid appeared to favor a close interaction between the surface of the membrane and the calcium ions of the water phase. We also visualized the bilayer from above (Fig. 2E, blue: positive charge, brown: negative charge) and found that the –OH was visible for all 3 HETE-PCs (red), facilitating the formation of a more negatively charged space, pushing headgroups apart, and making space for calcium to bind, in some cases near PS (pink) (Fig. 2E).

HETE-PE increases calcium membrane binding

To experimentally test for an interaction between calcium and HETE-PLs, we measured Fluo-FF fluorescence in the presence of liposomes, maintaining PC, PS, and total PE concentrations, but gradually replacing PE with 12-HETE-PE up to 10%. In this assay, lipid-dependent reduction of Fluo-FF fluorescence indicates elevated membrane calcium binding. In the presence of either 10 or 20 μM $CaCl_2$, control liposomes bound 1 or 2.5 μM calcium, respectively. This increased significantly with 3 to 10 % HETE-PE (Fig. 2F). These data support our hypothesis that HETE-PLs facilitate calcium binding on the surface of membranes to enhance PS-dependent clotting factor binding and activity.

HETE-PLs enhance coagulation and promote hemostasis in vivo

We next tested the ability of HETE-PLs to promote coagulation in vivo. For this, liposomes containing two different concentrations of 12-HETE-PE or 12-HETE-PC were injected intradermally into the tails of wild-type mice, immediately proximal to a tail cut. Control liposomes were without effect, whereas either 78 or 19 ng HETE-PL (per injection) significantly inhibited bleeding, in some cases leading to total cessation (Fig. 3A). Separately, i.v. injection of liposomes with 19 ng 12-HETE-PE into wild type mice significantly increased thrombin-antithrombin

complexes (TAT) (Fig. 3B). These data suggest that HETE-PLs are pro-coagulant in healthy mice in vivo. We measured eoxPL generation in vitro by platelets isolated from mice genetically lacking p12-LOX (encoded by the *ALOX12* gene). Washed platelets from wild type but not *ALOX12*$^{-/-}$ mice generated multiple isomers of 12-HETE-PE and –PC in response to thrombin activation (Fig. 3C, fig. S1). PLs with either plasmalogen or acyl bonds at the *Sn1* position, and also analogous eoxPLs from 22:4, 22:5 and 22:6 fatty acids were found, with all requiring p12-LOX activity (Fig. 3C). Time courses showed that HETE-PLs were already increased in abundance at 5 min, but continued to increase at least until 30 min after thrombin treatment (Fig. 3D).

Genetic deficiency of p12-LOX or 12/15-LOX leads to a bleeding defect that can be corrected with HETE-PE administration

To test the involvement of p12-LOX in regulating coagulation in vivo, we induced venous thrombosis with $FeCl_2$ in mice. In the $FeCl_2$ venous thrombosis model, a statistically significantly reduced thrombus weight was observed in *ALOX12*$^{-/-}$ mice (Fig. 4, A). Mice lacking either *ALOX12* (Fig. 4B) or *ALOX15* (Fig. 4C) also showed a significantly increased tail bleeding time, as well as increased blood loss, measured as hemoglobin (Hb) loss from the tail. We next tested whether administration of HETE-PLs restored hemostasis in the *ALOX12* or *ALOX15*$^{-/-}$ mice by administering small doses immediately proximal to a tail cut. Control liposomes containing 65% PC, 35% PE and 5% PS may be expected to have partial pro-coagulant activities depending on dose. Administration of 19 ng 12-HETE-PE in liposomes restored hemostasis back to that observed with wild-type amounts and was statistically significantly more effective than control liposomes at reducing bleeding time (Fig. 4, B and C).

Leukocyte and platelet HETE-PEs are increased in abundance in APS

To characterize HETE-PL generation in a human disease associated with venous thrombosis, HETE-PEs were quantified in isolated platelets and leukocytes from patients with antiphospholipid syndrome (APS) and healthy controls (tables S1 and S2). We detected statistically significantly-increased basal concentrations of 5-HETE-PE (from neutrophils, monocytes, via 5-LOX) and 15-HETE-PE (from eosinophils, via 15-LOX) in leukocytes from APS patients compared to the amounts detected in cells from healthy volunteers (Fig. 5, A and B). After the activation of leukocytes with a calcium ionophore. HETE-PEs increased in abundance in both groups to a similar extent (Fig. 5, A and B). This suggests that leukocyte LOXs generate HETE-PEs basally in APS. The lack of difference between healthy controls and APS after stimulation with ionophore could imply that 15- and 5-LOX abundances are similar in leukocytes from both groups, although HETE-PL generation also depends on arachidonic acid (AA) substrate availability and the rate of re-esterification into lysoPLs. Platelets from APS patients contained statistically significantly more 12-HETE-PE than did those from healthy controls, both basally and after thrombin activation (Fig. 5C).

Our methods are optimized so that spontaneous activation is minimized during platelet isolation, specifically by using a wide-bore needle, ensuring a constant room temperature, and minimizing the numbers of wash steps and manipulations performed. Despite these steps, platelets from APS patients tended to spontaneously aggregate during isolation. Specifically, no platelets from healthy subjects aggregated until challenged with thrombin, whereas of the platelets from 12 APS patients, 9 appeared to at least slightly aggregate during the last washing step of platelet isolation. Of those, 7 generated a platelet "clot" that we removed and analyzed separately. Thus, our data suggest that platelets from APS patients are inherently more "poised" to activate. The amount of 12-HETE-PE in these spontaneously aggregated platelets was similar to the amounts in thrombin-activated APS platelets (Fig. 5, C and D), suggesting that they also generated increased amounts. We confirmed increased platelet activation in vivo in APS by measuring 11-thromboxane B2 (TXB_2), a urinary

metabolite of thromboxane A2 formed by platelet COX-1 (Fig. 5E). The increased TXB_2 abundance in urine is consistent with platelets from APS patients circulating in a heightened activation state in vivo.

Next, we next analyzed leukocytes for platelet-derived 12-HETE-PEs and platelets for leukocyte-derived 5- and 15-HETE-PEs. 15- and 5-HETE-PEs were increased basally in platelets from APS patients (Fig. 5, F and G). Unlike 12-HETE-PEs, these did not show a statistically significant increase in abundance in response to thrombin, indicating they were not from platelets. Instead, 15- and 5-HETE-PEs on the platelets could represent microparticles from other cells that had attached to the platelets. Leukocytes from APS patients had increased amounts of platelet 12-HETE-PEs compared to those of controls, and this lipid increased further upon ionophore activation (Fig. 5H). Thus, platelets or platelet-derived microparticles may be associated with APS patient leukocytes during isolation and may remain responsive to ionophore activation in vitro. It is well known that platelet-derived microparticles are increased in number in APS (28), and we previously showed that 12-HETE-PE and –PC are present in vesicles generated by thrombin-activated platelets in vitro (10,29). Most of the patients were taking anti-coagulant medication; thus, an influence of this on eoxPLs cannot be excluded (table S1). Although samples sizes were small, gender, age, and concurrent arterial thrombosis did not appear to influence eoxPL amounts (fig. S2, table S2).

APS patients have increased amounts of plasma IgG directed against HETE-PEs

We sought to determine whether HETE-PLs acted as an antigen for antibodies in APS by measuring the amount of IgG specific for HETE-PE compared with the amount of IgG specific for the unoxidized analog, 1-stearoyl-2-arachidonyl-PE (SAPE). APS serum had a substantial increase in the amount of IgG recognizing 5-, 12- and 15-HETE-PEs (Fig. 6, A to C). IgG against SAPE was also increased, but this was not statistically significant. Total IgG was comparable between both

groups (Fig. 6D). This suggests that chronic higher exposure to HETE-PEs leads to the enhanced immune recognition of these lipids in patients.

HETE-PEs enhance APS-associated plasma protein binding to the cellular surface

β2GPI is a positively charged protein that binds to anionic PLs, such as cardiolipin, resulting in a conformational change that exposes cryptic epitopes recognized by pathogenic disease-associated antibodies (14). This interaction is believed to result in downstream signaling with a net pro-coagulant effect. Because HETE-PLs can enhance calcium binding (Fig. 2F), we tested whether they also increased β2GPI interactions with the plasma membrane using PS and PC containing-liposomes. Binding of human purified β2GPI was enhanced by cardiolipin, or on substitution of PE with 15-HETE-PE (Fig. 6E). Also, 5- or 12-HETE-PE increased the cardiolipin-dependent binding of β2GPI binding to the liposome in comparison to HETE-PEs or cardiolipin alone (Fig. 6F). Thus, HETE-PEs enhance the binding of β2GPI to membranes, a process that is required for the protein to become antigenic.

Lipidomics defines the complexity of eoxPL enzymatic generation in human platelets, including previously uncharacterized control networks

More than 100 eoxPLs are generated by thrombin-activated human platelets (11-13). The enzymatic origin of most of these lipids is not defined. Here, the 47 most abundant lipids were profiled in patients from healthy controls and APS patients (both unstimulated and after thrombin activation) to examine their behavior in the context of a thrombotic disease (Fig. 7A, fig. S3). Where the enzyme responsible for synthesizing the lipid was known, lipids were labeled as being derived from either COX-1 (blue) or p12-LOX (red) (Fig. 3 D), based on our observation of their absence in *ALOX12*$^{-/-}$ mouse platelets or having a known sensitivity to aspirin, which define PGE_2- or DXA_3-PEs that are produced by COX-1(11,12)(. Cluster analysis revealed two prominent groups of related lipids

visible based on COX-1 or p12-LOX. Several polyhydroxylated lipids grouped with COX-1, suggesting they may also originate from that pathway (green), and five mono-hydroxylipids (black) grouped with p12-LOX. Note that eoxPL clustered strongly based on the *Sn2* fatty acid, with hydroxydocosahexanoic acids (HDOHEs), HETEs, and monohydroxy C22 lipids forming associated groups. From visual inspection, 12-LOX–derived lipids appeared to increase in abundance to a greater extent than did other lipids in response to thrombin, and are increased in abundance in the APS patients compared to the healthy controls.

Next, we plotted correlations between lipids (i.e. how each lipid behaved in relation to others individually) to further examine their behavior within the APS cohort (Fig. 7B). Here, lipids were sorted by decreasing correlation with 18:0a/12-HETE-PE, an abundant eoxPL that is generated by p12-LOX. p12-LOX– and COX-1-derived lipids grouped together, with polyoxygenated lipids correlating more closely with COX-1. However, this visualization also revealed a family that correlated with 16:0e/22:5(O)-PE (red arrows, and table) (Fig. 7B, fig S4). Note that almost all were acyl-PEs and PCs, with exclusively either 22:5 or 22:4 monoxygenated fatty acids at *Sn2,* and several were p12-LOX–derived. This suggests that 12-LOX forms 22:4(O) or 22:5(O) PLs that are regulated as a group. Together with the hierarchical cluster analysis (Fig. 7A), this further supports the idea of differential behavior based on the composition of the *Sn2* oxidized fatty acid.

For both the cluster analysis and correlation analyses, we normalized all lipids to the mean of the control unstimulated values. Thus, we could examine how each lipid behaved individually, relating to activation or health and disease. There are major differences in abundance between individual lipids, e.g. HETE-containing PLs predominate, whereas lipids from less abundant fatty acids or with multiple oxygens are present in lower amounts (11-13). If data are not normalized, then correlations will be influenced by amounts rather than biological pathways. We also generated correlations in

which we separated the APS and healthy control datasets (fig. S5). Whereas these appeared to be visually distinct, the same trends whereby 12-LOX–derived lipids or COX-1/polyoxygenated lipids correlated in groups based on biological pathway was maintained.

We then characterized the 47 lipids using a network analysis (Cytoscape 3.2.1), in which nodes represented individual lipids and node size was determined by the number of links to other lipids (Fig. 8A). Edge thickness represented the strength of correlation between individual nodes. Nodes with the highest degree clustered toward the center. The network diagram illustrates that the COX-1– and p12-LOX–derived lipids behaved as two separate groups, with only a small degree of relatedness between them. The analysis further showed that all remaining 20:4(3O) lipids located with COX-1, suggesting that they are prostaglandin (PG)-containing PLs. Four PEs correlated with p12-LOX, indicating this as their origin. When analyzed as a single group, the 31 p12-LOX derived eoxPLs were statistically significantly increased in abundance in APS platelets both basally and after thrombin stimulation, whereas for COX-1–derived eoxPLs, a trend towards increased amounts in APS was noted (Fig. 8B). Last, a group of exclusively plasmalogen mono- or dioxygenated-PEs from 22:5 or 20:4 behaved as a separate family, suggesting that they have a different enzymatic origin than from either COX-1 or p12-LOX (Fig. 8 A). Unlike COX-1– and p12-LOX–derived eoxPLs, these lipids did not exhibit an increase in abundance upon thrombin activation and were present basally (fig. S3). It is also noteworthy that COX-1–derived eoxPLs are almost exclusively plasmalogen PE species, whereas p12-LOX-derived eoxPLs include both acyl and plasmalogen forms, as well as PC and PE.

Discussion

Herein, we showed using in vitro coagulation studies, murine venous thrombosis models, and MD simulations that HETE-PLs increase the activities of calcium/PS-dependent factors in vitro and in

vivo (Figs. 1 to 4). Coagulation factors associate with anionic phospholipids (classically, native PS and PE) through interactions with positively charged calcium ions. Positioning the HETE hydroxyl group near the membrane surface appears to enhance this and provides a mechanistic basis for our observations (Fig. 2). Mice lacking either *ALOX15* (leukocyte-type 12/15-LOX, or 15-LOX) or *ALOX12* (platelet-type 12-LOX) were affected in venous bleeding challenge models, suggesting that both LOX isoforms likely act in concert to achieve effective hemostasis in vivo (Fig. 4). Circulating blood cells from patients with the thrombotic disorder APS had substantially greater amounts of leukocyte- and platelet-derived eoxPLs basally, in concert with enhanced anti-HETE-PL immunoreactivity (Figs. 5 to 6). Furthermore, by undertaking a comprehensive lipidomics analysis of platelets from APS patients and controls, a complex network of independently regulated eoxPL families from COX-1 and p12-LOX was revealed (Figs. 7 to 8). A large group of platelet lipids, generated by p12-LOX, were substantially increased in abundance in APS (Fig. 8B). Together, these data are suggestive of a contribution of eoxPLs from this pathway to human thrombotic disease through their procoagulant or immunogenic activities, but this remains to be conclusively proven. The clear stratification of lipids into groups that behaved differently based on headgroup, *Sn2* fatty acid, or *Sn1* acyl/plasmalogen composition shown by the clustering and network analyses suggests additional enzymatic regulation mechanisms for eoxPL formation and metabolism in platelets, which remain to be characterized. These could include differential enzymatic control of acylation of the oxidized fatty acids into specific lysoPL species. In this regard, little is yet known about fatty acyl CoA ligase or lysophospholipid acyl-transferase isoform preference for different oxidized fatty acids or eicosanoids as substrates for esterification, in platelets or any cell type.

Previous studies proposed a role for lipid oxidation in APS, because non-enzymatic oxidation products are increased in abundance in urine (30). We suggest that this may be initiated by

leukocyte and platelet LOXs, with primary enzymatic oxidation products, such as peroxides and lipid radicals, decomposing and mediating propagation reactions non-enzymatically. Although there are numerous antigenic targets for antiphospholipid antibodies, only some have been implicated in APS (31,32). Further study is necessary to determine whether HETE-PE–specific antibodies are causally involved; however, increased amounts of IgG indicate that the lipids would likely be chronically increased in abundance in APS patients with thrombotic disease.

A mechanism proposed to promote thrombosis in APS involves increased binding of β2GPI to PF4, causing platelet activation that is indicated by the measurement of increased TXB_2 amounts in vivo (33-35). In this regard, we found the HETE-PEs facilitated increased β2GPI binding to membranes, both directly and through enhancing cardiolipin-dependent binding, and we also observed increased amounts of TXB_2 in our cohort of APS patients compared to those in controls (Fig. 5E, 6, E and F). In addition, APS monocytes can promote both coagulation and inflammation through the production of increased amounts of tissue factor (TF), TNF-α, and IL-1 (36,37). The binding of β2GPI to monocytes in complex with anti-β2GPI IgG increases the production of TF (38). Thus, our studies suggest two potential mechanisms for increased thrombosis linked to eoxPLs: (i) direct HETE-PL enhancement of PS-dependent coagulation on the platelet or leukocyte surface by the mechanisms characterized herein, and (ii) increased β2GPI binding to oxidized phospholipids on the surface of circulating immune cells, which in turn promotes inflammation and TF production. Further work is required to determine the relative contributions of these mechanisms to APS. We also noted a substantial increase in the amounts of neutrophil 5-LOX-derived 5-HETE-PE and 5-HETE-PE IgG, which suggests that these cells circulate in an activated state in APS (Figs. 5B, 6B) (39). Because 5-HETE-PE also increased cardiolipin-dependent β2GPI membrane binding, potentially mimicking apoptosis, this could enhance the neutrophil activation and clearance that is characteristic of APS (Fig. 6E) (40).

Coagulation factors FII, VII, IX and X contain Gla domains, specialized regions that contain posttranslational modifications of many glutamate residues by vitamin K–dependent carboxylation to form □-carboxyglutamate. These mediate a high-affinity interaction of calcium with cell-surface aPL, particularly PS and PE (2,23). The cofactors FVIII and FV bind to negatively charged phospholipids through the homologous C1 and C2 domains. HETE-PLs enhanced coagulation in vitro and in vivo (Figs. 1,3,4). Native PC alone does not support coagulation, because its bulky head group inhibits Gla domain interactions with its phosphate (2). However, in multiple experiments in vitro and in vivo, we found that HETE-PC promoted coagulation (Fig. 1, D to F, 3A). Most previous studies have focused on the head group; however, PLs also differ with respect to fatty acid composition (3,26). Thus, the action of an eoxPL is entirely dependent on the oxidized epitope. This represents a paradigm shift in our understanding of hemostasis, whereby certain forms of PC rapidly generated by activated leukocytes and platelets promote clotting. Determining which specific factors and co-factors are sensitive to HETE-PLs will be undertaken using recombinant factors and surface plasmon resonance in a follow-up study.

HETE-PLs directly enhanced PS-dependent thrombin generation, suggesting that they act similarly to native PE through calcium binding (Fig. 1, G to J). Our molecular dynamics simulation supports this (Fig. 2). The HETE-hydroxyl group quickly moved near-to the surface of the membrane, where it interacted with calcium. It also increased the distance between the headgroups, enabling greater accessibility to the phosphate group. To some extent, the effect of HETE-PL mimics the role of the carboxylic acid of the PS headgroup, which offers an anchor to calcium, and this idea is supported by our demonstration of an increased calcium association with HETE-PE liposomes (Fig. 2F). This process also provides a potential explanation for the enhanced binding of β2GP1 to membranes. Cardiolipin is negatively-charged at pH 7.4. Although it contains two phosphate groups, the pKa

values are such that one is protonated and one is not at pH 7.4, giving cardiolipin an overall net negative charge. We hypothesize that in a similar way to PS, through pushing upwards, the HETE group may enable the cardiolipin phosphates to interact more effectively with the positively charged β2GP1.

The concentrations of HETE-PLs in thrombinoscope assays ranged from 10 to 100 ng/ml. We calculated the amounts of HETE-PL generated by human and mouse platelets to be 23 ng/4 x 10^7cells and 35 ng/2 x 10^8 platelets, respectively (9) (Fig. 3D). Given typical blood platelet concentrations (2 or 4 x 10^8/ml for human or mouse, respectively), this would be expected to equate to around 120 ng/ml or 70 ng/ml of HETE-PLs for mouse or human blood. HETE-PE and HETE-PC isomers represent only a proportion of the total phospholipid oxidation products that form during platelet activation, with more than 100 individual molecular species being formed acutely (13). Thus, the actual concentration of potential pro-coagulant eoxPLs in the platelet membrane is likely to be considerably greater than our estimates. Furthermore, studies showed that annexin V binding is clustered to discrete domains of the activated platelet membrane, where procoagulant PLs concentrate, thus achieving even greater local amounts (41).

ALOX12$^{-/-}$ mice have increased venous tail bleeding (42,43). We showed that hemostasis is restored in both *ALOX12* and *ALOX15*$^{-/-}$ mice through administering liposomes that promote clotting factor activities in vitro and increase TAT abundance in vivo. Because liposomes themselves do not aggregate, this indicates that they act solely through providing a pro-coagulant surface. These data support the idea that coagulation is defective in these mice (Fig. 4 C,D). The earliest study on *ALOX12*$^{-/-}$ mice reported normal platelet aggregation in response to most agonists, with a slight hyper-responsiveness to ADP, indicating no functional deficit (44). Venous thrombosis as studied herein is predominantly dependent on coagulation, rather than platelet function. In this regard, APS

venous thrombosis responds best to anticoagulation therapies (e.g. warfarin and heparin) but less well to antiplatelet therapies (such as aspirin and clopidogrel). Although our data suggest that eoxPLs may contribute to the thrombotic phenotype in APS in the absence of orally active LOX inhibitors and with the patients on oral anticoagulant therapy, it is not currently possible to test this conclusively.

We used eoxPLs generated by chemical or air oxidation that were purified by HPLC, because it is not currently possible to use enzymes to generate sufficient amounts for biological studies (except for 15-HETE-PE). Regardless of how the lipids are generated, they will be virtually identical, with the only difference being enantiomeric composition. Specifically, mammalian immune cell LOXs generate the S enantiomer, whereas air or chemical oxidation results in an approximately 50:50 mixture of S and R enantiomers. In the case of our biological studies, where pro-coagulant activity is not based on a receptor dependent effect and is instead related to electronegative character, we do not expect S or R enantiomers to differ. Indeed, our observation that several positional isomers and both PE and PC forms were pro-coagulant supports this idea.

In summary, we demonstrated that families of eoxPLs increased in abundance during APS provide an immunogenic target, a binding site for β2GPI, and promote coagulation in vitro and in vivo. We also characterized the mechanism by which they enhance coagulation and showed their ability to support normal hemostasis in mice. Using lipidomics and correlation networks, we uncovered enzymatic control pathways for multiple families of eoxPLs generated by activated platelets. The findings define mechanisms by which physiological membrane oxidation regulates innate immune cell function during acute activation or inflammation, and may lead to the development of new diagnostic tools or treatments for bleeding or thrombotic diseases.

Materials and Methods

Reagents

Corn trypsin inhibitor (CTI, recombinant) and full-length tissue factor (TF, human recombinant) were from Haematologic Technologies Inc. FII Fluorogenic substrate (Z-Gly-Gly-Arg-AMC) was from Bachem (St Helens, UK). T-cal Thrombinoscope calibrator was from Stago. 1-Stearoyl-2-arachidonoyl-phosphatidylethanolamine, -phosphatidylcholine and -phosphatidylserine (SAPE, SAPC, SAPS) and 1,2-di-stearoyl-phosphatidylcholine (DSPC) were from Avanti Polar Lipids. 2,2'-Azobis(4-methoxy-2,4 dimethyl-valeronitrile) (MeOAVM) was from WAKO. All other chemicals and lipsofast membranes were from Sigma-Aldrich, except for N-methyl Benzohydroamic acid (NMBHA), which synthesized in-house as previously described (45). Solvents were from Fisher Scientific. HETE-PEs and –PCs were generated and purified as previously described (46).

Study design

All studies were carried out in accordance with the principles of the Declaration of Helsinki and with informed consent and full ethical approval. Antiphospholipid syndrome: The study was approved by the South West Wales Research Ethics Committee (12/WA/0229). Patients (total 18) with APS associated with venous thrombosis were recruited from haematology clinics. All had at least one incidence of venous and/or arterial thrombosis and tested positive for at least one laboratory criterion (Lupus anti-coagulant and/or high anti-cardiolipin IgG titres and/or high anti-β2GPI IgG titres measured on two occasions at least 12 weeks apart). Patients were not taking aspirin or other non-steroidal anti-inflammatory drugs at the time of venepuncture. Most were taking anti-coagulants, for example, warfarin or rivaroxiban, none had diabetes, and only one had high cholesterol at the time of sampling. Full details on all patients are shown in table S1. Blood samples were collected from patients following a routine clinical visit, in a quiescent state with no clinical

thrombotic episode at the time of sampling. Healthy controls (total 34) were recruited from the local population and were excluded if they had a history of arterial or venous thrombosis, recurrent fetal loss, cardiac disease or any other chronic inflammatory diseases such as rheumatoid arthritis, SLE, diabetes, high cholesterol, abnormal renal or liver function, or other diseases that may conflict with the study parameters. Individuals within the HC group had not taken aspirin, non-steroidal anti-inflammatory drugs or any other medication in the preceding 14 days. Informed consent was obtained from all participants. Age and gender demographics are given in table S2. Blood samples were collected from APS patients and healthy controls via venepuncture from the median cubital vein. Full blood counts (FBC) were collected, any patients or healthy controls with an abnormal FBC at the time of sample collection were retrospectively omitted from the study. Washed platelets and leukocytes were then isolated and activated. Serum, plasma and urine were also collected. Blood donations from healthy volunteers were approved by the Cardiff University School of Medicine Ethics Committee, and were with informed consent (SMREC 12/37, SMREC 12/10). A power calculation was not undertaken because preliminary data was not available for our studies. Rules for stopping data collection were not defined. Outliers were not removed and endpoints were not prospectively selected. Replicates for all experiments are included in figure legends. The objectives of the research were to define whether eoxPLs could modulate coagulation reactions, determine the mechanisms involved, and examine whether eoxPLs were increased in human thrombotic disease. Research subjects included patients with APS (total number 18) and healthy controls (total number 34), mice (wild type and genetically modified) and liposomes of defined composition. There were several different studies in our design, including controlled laboratory experiments and observational studies. Randomization is not relevant as we did not conduct a clinical trial. Blinding was used during analysis of lipids from patients and controls, but not in animal, cellular or liposome experiments.

Generation of liposomes

Liposomes were made by freeze-thawing followed by extrusion in 20 mmol/L HEPES, 100 mmol/L NaCl, pH 7.35 (buffer A). Where HETE-PE was substituted for unoxidized PE, the liposomes used were: 5 % SAPS, 20 to 30 % SAPE, 0 to 10 % HETE-PE, and 65 % DSPC (mol %). Where unoxidized PC was substituted for HETE-PC the liposomes used were: 5 % SAPS, 30 % SAPE, 55 % DSPC, 0 to 10 % SAPC, and 0 to 10 % HETE-PC. Liposomes were made in the presence of 10 pmol/L full length recombinant TF, and used at a final concentration of 4 μM total lipid unless otherwise stated. Binding of β2GP1 to liposomes was also determined.

Thrombin generation assays

Thrombin generation assays were performed using a Fluoroskan Ascent plate reader (ThermoLabsystems, Helsinki, Finland). Cleavage of prothrombin to thrombin was measured using 0.5 mmol/L fluorogenic substrate Z-Gly-Gly-Arg-AMC and thrombin activity was compared to the thrombin calibrator (Stago). Thrombin generation was calculated from raw fluorescence data as described previously (47). Cleavage of prothrombin to thrombin in simplified coagulation cascade experiments was performed according to the same methods but using a mixture of FII (1.4 μmol/L), FV (26 nmol/L), FVII (10 nmol/L), FVIII (300 pmol/L), FIX (80 nmol/L), and FX (136 nmol/L) in buffer A with 1 % BSA (buffer B). The reaction was initiated by the addition of $CaCl_2$ (20 mmol/L) and fluorogenic substrate (0.5 mmol/L) in buffer B.

Lipid extraction and analysis

1,2-dimyristoyl-PE or -PC (10 ng) was added to each sample before extraction as an internal standard. Lipids were extracted by adding a solvent mixture [1 M acetic acid, 2-propanol, hexane (2:20:30)] to the sample at a ratio of 2.5 ml solvent mixture to 1 ml sample, vortexing, and then adding 2.5 ml of hexane. Following vortexing and centrifugation (400 g, 5 mins), lipids were

recovered in the upper hexane layer. The samples were then re-extracted by the addition of an equal volume of hexane followed by further vortexing and centrifugation. The combined hexane layers were then dried under vacuum and analyzed for HETE-PE using LC/MS/MS. Samples were separated on a C_{18} Luna, 3 μm, 150 mm x 2mm column (Phenomenex) gradient of 50-100 % solvent B for 10 min followed by 30 min at 100 % B (Solvent A: methanol:acetonitrile:water, 1 mM ammonium acetate, 60:20:20; Solvent B: methanol, 1 mM ammonium acetate) with a flow rate of 200 μl/min. Electrospray mass spectra were obtained on a Q-Trap instrument (Applied Biosystems 4000 Q-Trap) operating in the negative mode. Products were analyzed in the MRM mode monitoring transitions from the parent ion to daughter ion of 179.1 (12 HETE $[M-H]^-$) every 200 ms with a collision energy of -45 to 42V. The area under the curve for the parent ion to the 179.1 ion was integrated and normalized to the internal standard for 16:0p, 18:1p/ 18:0p and 18:0a/12-HETE-PEs. For quantification of these lipids, standard curves were generated with purified 18:0a/12-HETE-PE/PC. Where large numbers of HETE-PLs were measured in lipidomics assays, fold changes relative to PE or PC internal standards were determined using MRM transitions from a previous study (13).

Liposome composition for β2GP1 binding experiments

All liposomes were as described earlier after extrusion, but with the following lipid composition: 55% distearoly-PC (DSPC), 15 % stearoyl-arachidonyl-PS (SAPS), 10 % stearoyl-arachidonyl-PC (SAPC), 1 % stearoyl-arachidonyl-PE-biotin (SAPE-B, generated by reacting NHS-biotin with PE and purification using HPLC), 19 % stearoly-arachidonyl-PE (SAPE). In some experiments, an equivalent amount of SAPE was replaced with 1 % 15-, 12- 5-HETE-PE, and/or 1 % cardiolipin. Liposomes were immobilized onto Polysorp plates (Nunc) coated with 5 μg/ml Neutravidin. 1 μg/ml β2GPI was added for 1 hour at room temperature. Bound β2GPI was determined using anti-

β2GPI-HRP antibody (1:20,000) (Cedarlane) and ECL detection (Pierce). Data are expressed as the relative light units per 100 ms (RLU/100 ms).

Determination of circulating antibodies to HETE-PEs

Specific antibody titers to individual HETE-PEs were determined by chemiluminescent ELISA as previously described (48). Lipids were coated onto Microfluor plates at 20 μg/ml and subsequently blocked with 0.5% fish-gelatin in 0.27 mM PBS-0.27 mM EDTA. EDTA plasma samples (1:12) were diluted in PBS-0.27 mM EDTA and incubated for 1 hour at room temperature. The bound IgG was measured using an anti-human IgG alkaline phosphatase-conjugated secondary antibody (Sigma Aldrich) and LumiPhos 530 (Lumigen, Inc). Data are expressed as the relative light units per 100 ms (RLU/100 ms).

Isolation of human washed platelets

Washed platelets were prepared from whole blood drawn from a central venous catheter into syringes containing acidified citrate dextrose (ACD; 85 mM trisodium citrate, 65 mM citric acid, 100 mM glucose) at a ratio of 8.1 parts whole blood to 1.9 parts ACD, as described previously (46), and resuspended in modified Tyrode's buffer (134 mM NaCl, 12 mM $NaHCO_3$, 2.9 mM KCl, 0.34 mM Na_2HPO_4, 1.0 mM $MgCl_2$, 10mM HEPES, 5mM glucose, pH 7.4) at 2 x 10^8/mL. Platelets (1 ml) were incubated at 37 ^oC for 30 min with 1 mM $CaCl_2$, 0.2 U/mL human thrombin (Sigma-Aldrich, UK) or modified Tyrode's buffer.

Isolation of human leukocytes

Leukocytes were isolated from 20 ml citrate anticoagulated whole blood. Briefly, 20 ml of whole blood was mixed with 4 ml of 2 % citrate and 4 ml of Hetasep (Stem Cell Technologies) and allowed to sediment for at least 45 minutes. The upper plasma layer was recovered and centrifuged at 250

g for 10 min at room temperature. The pellet was resuspended in ice-cold 0.4 % trisodium citrate/PBS and centrifuged at 250 g for 5 min at 4 °C. Erythrocytes were removed by hypotonic lysis. Leukocytes were resuspended in Krebs buffer at 4 x 10^6/ml. Leukocytes were activated at 37 °C with 10 μM A23187 in the presence of 1 mmol/$CaCl_2$, for 30 min, prior to lipid extraction.

Isolation of serum, plasma and urine

Blood was collected into EDTA, Lithium-Heparin, or Citrate vacutainers prior to centrifugation at 900 g. The plasma layer was collected and centrifuged again at 900 g to remove any residual platelets. Plasma was stored at -80 °C for use in *in vitro* assays. Whole blood was collected into a clot-activating vacutainer and centrifuged at 900 g. The serum was collected and centrifuged again at 900 g to remove any residual cells. Serum was stored at -80 °C for use in *in vitro* assays. Urine was collected into universal containers, samples were aliquoted and stored at -80 °C until use.11-dehyro-TxB_2 was measured using GC/MS as previously described (49).

Isolation and activation of mouse washed platelets

Mouse blood was obtained by cardiac puncture directly into a syringe containing 150 μl ACD (2.5% w/v trisodium citrate, 1.5 % w/v citric acid, 100 mM glucose). The syringe was emptied into an eppendorf tube containing 150 μl 3.8 % w/v sodium citrate, and 300 μl of modified Tyrode's buffer was then added (145 mM NaCl, 12 mM $NaHCO_3$, 2.95 mM KCl, 1 mM $MgCl_2$, 10 mM HEPES, 5 mM Glucose). The blood was spun for 5 min at 150 g at 25 °C, and platelet-rich-plasma (PRP) was removed. Another 400 μl of Tyrode's buffer was added, carefully mixed into the blood without inverting the tube, and more PRP was removed after a second, identical, spin. A third spin at 530 g for 5 min on the pooled PRP pelleted the platelets, plasma was removed, and the platelets were re-suspended in Tyrode's buffer at 2 x 10^8 ml^{-1}. Half of the platelets were used as unstimulated controls,

and the rest were activated with 0.2 U/ml thrombin and 1 mM $CaCl_2$ followed by gentle mixing every 2 - 3 min for 30 min at 37 °C.

Thrombin-Antithrombin (TAT) complex measurement

Whole blood was collected via a cardiac puncture into one-tenth volume of 3.8 % sodium citrate as an anticoagulant and centrifuged at 3,000 x g for 10 min. Plasma thrombin-antithrombin (TAT) amounts were determined using a commercially available enzyme-linked immunosorbent assay kit (Mouse Thrombin-Antithrombin Complexes ELISA Kit; ab137994, abcam).

Quantification of blood loss from tail bleeding assays

C57/BL6 wild type (Charles River), *ALOX15*$^{-/-}$ and *ALOX12*$^{-/-}$ mice bred in-house were kept in constant temperature cages (20 – 22 °C) and given free access to water and standard chow. Tail bleeding assays and breeding of mice was performed under Home Office Licence PPL/3150. Male mice (11 week old) were anesthetized using 5 % isoflurane and maintained with 2 % isoflurane. Where administered, liposomes [10 µl generated as described earlier, using either (i) 30 % SAPE, 65 % DSPC, 5 % SAPS, and 2.5 nmol/L TF, or (ii) 20 % SAPE, 65 % DSPC, 5 % SAPS, 10 % 12-HETE-PE and 2.5 nmol/L TF) were injected immediately proximal of the cut site directly before transection of 2 - 5 mm from the distal end and immediate immersion in 37 °C physiological saline. Bleeding was observed as blood loss and time to the beginning of stable (1 min) cessation of blood flow determined, before killing via cervical dislocation. Blood loss was quantified by measuring the hemoglobin (Hb) content of the saline, as follows. Hemoglobin quantitation was achieved via centrifugation of the tube at 250 x g for 15 min, and resuspending the red cells in 5 ml erythrocyte lysis buffer (8.3 g/L NH_4Cl, 1 g/L $KHCO_3$ and 0.037 g/L EDTA in distilled H_2O). The concentration of Hb was measured as optical density (OD) 575 nm using a UVIKON 923 double beam UV /VIS spectrophotometer (Bio-Tek Kontron Instruments) and expressed as absorbance units (AU).

Injury-related venous thrombosis

Thrombosis was induced as described previously with minor modifications (50). In brief, mice (20 - 25 g body weight) were anaesthetized with ketamine (100 mg/kg body weight) and xylazine (20 mg/kg body weight), and placed under a heating lamp to maintain a constant body temperature of 37 °C. A ventral midline incision was performed and the intestines were gently put aside. The inferior vena cava was laid free carefully and a filter paper (1 mm x 2 mm x 4 mm) soaked with 4 % of aqueous ferric chloride solution was placed on top of the vessel. After 3 min, the filter paper was removed and the peritoneal cavity thoroughly rinsed with pre-warmed 0.9 % saline. After another 30 min, mice were sacrificed, blood was taken by cardiac puncture, and the vena cava containing the thrombus removed. The clot was dissected free from the vessel and prepared under a microscope for further analysis. Wet thrombus weight was measured using a precision balance (Sartorius R16P) after removal of excess water.

Lipid Bilayer Model Preparation, and membrane energy minimization and simulation protocol

A pre-equilibrated hydrate lipid bilayer consisting of 128 molecules of 1,2-Dioleoyl-sn-glycero-3-phosphocholine (DOPC), based on a previously reported study, was downloaded from the ATM database (Box ID: 30) (51,52). The lipid bilayer was structurally modified by removing DOPC using the MOE (53) builder tools according to the experimental composition of the tested liposomes to give the following composition: 5 % SAPS, 5 % SAPC, 30 % SAPE, 55 % DOPC, 5 % 12-HETE-PC. Initially, a conformational analysis of 12-HETE-PC was performed with two different low energy conformations included in the membrane. The first conformation presented the oxidized lipid chain in an elongated structure and was used for the three 12-HETE-PCs in one monolayer. The second presented the oxidized chain in a bent conformation and was used in the other monolayer.

As a result, the 12-HETE-PC presented the hydroxyl groups differently on the two different membrane layers: on one side, the hydroxyl groups were placed deep in the membrane, whereas on the other side, they were close to the membrane surface. All the modified lateral chains were minimized in MOE using an OPLS-AA force field with a gradient of 0.1Kcal/mol/Å^2. Hydrate membrane energy minimization and simulation were performed by using Desmond (Maestro interface) with OPLS_2005 set of force field parameters (54,55). The TIP3P water model was used and the assembled system consisted of 35426 atoms enclosed in a 69 x 70 x 80 Å^3 triclinic box. 14 molecules of $CaCl_2$ were added as salt. Energy minimization of the system was run with a steepest descent until a gradient threshold of 25 kcal/mol/Å was reached. A 300-ns molecular dynamics (MD) simulation was then performed using the Desmod default parameters with the temperature set to 300 K, pressure set at 1.01325 bar, and the time step was set to 2 fs. Energy of the simulation was recorded every 120 ps, whereas the trajectory was recorded every 480 ps.

Measurement of calcium binding to membranes

Glass tubes were pre-washed using 1 M hydrochloric acid and methanol. All buffers were treated with 10 mg/ml pre-washed chelex-100 and kept in plasticware to reduce calcium contamination to 1 - 2 μM. Liposomes containing 65 % DSPC, 30 % SAPE, 5 % SAPS liposomes, or with SAPE replaced with up to 10 % 15-HETE-PE were prepared in potassium phosphate buffer. The free calcium concentration in the samples was measured using 1 μM Fluo-FF calcium dye (Kd 9.7 μM, ex 485 nm, em 520 nm), with 10 or 20 μM calcium added. Decreases in free calcium in lipid solutions compared to the buffer blank represent membrane-bound calcium. A standard curve for Fluo-FF response was constructed using 10 mM nitrilotriacetic acid (Kd 78.6 μM) as calcium buffer, that is,

$$[Ca^{2+}]_{membrane} = [Ca^{2+}]_{total} - [Ca^{2+}]_{free} - [Ca^{2+}]_{Fluo\text{-}FF\ bound} - [Ca^{2+}]_{contaminants}$$

and for the buffer blank:

$$[Ca^{2+}]_{total} = [Ca^{2+}]_{free} - [Ca^{2+}]_{Fluo\text{-}FF\ bound} - [Ca^{2+}]_{contaminants}$$

Heatmap and Cytoscape correlation

Heatmaps were generated using the pheatmap package in R using hierarchical clustering (complete linkage method) to group similar lipids (version 3.3.1). Data were first normalized to the mean of the unstimulated control values for each lipid. Network analysis was performed with Cytoscape (version 3.4.0), using pairwise correlations between lipids generated with R. The network diagram shows only correlations with a Pearson product-moment correlation coefficient value (r) > 0.8 because of the high number of interactions.

Statistical analysis

Statistical significance was calculated with the Mann Whitney U test, unless otherwise stated. The statistical differences between β2GPI binding to HETE-PL and cardiolipin liposomes were calculated by one-way ANOVA with Tukey-Kramers multi-comparison post hoc test, which was used to compare the means of each condition. Statistical significance is denoted as follows: $*P < 0.05$; $**P < 0.01$; $***P < 0.001$. Statistical analysis was performed using Graphpad Prism 6. Unless otherwise stated in figure legends, data were displayed as tukey boxplots, where whiskers represent 1.5 the lower and upper interquartile range, data not included within the whiskers is displayed as individual outliers. The correlation plot (Fig. 7B) was created in R using the corrplot package (56,57).

Supplementary Materials

Fig. S1. Primary data for the generation of eoxPLs by washed WT and *ALOX12*$^{-/-}$ platelets.
Fig. S2. Analysis of HC and APS demographics for effects on eoxPL generation shows no effect of age, gender, or arterial thrombosis on platelet 12-HETE-PEs.
Fig. S3. Primary data for the generation of eoxPLs by washed platelets from HCs and APS patients.
Fig. S4. Correlation plots for lipids from all groups shows that lipids group according to enzymatic origin.
Fig. S5. Correlation plots for lipids from either HCs or APS patients shows that lipids group according to enzymatic origin.
Table S1. Patient demographics and relevant medical details.

Table S2. Age and gender demographics of study participants.
Movie S1. Simulation of the movement of HETE-PC in a lipid biomembrane.

References and Notes

1. Falls, L. A., Furie, B., and Furie, B. C. Role of phosphatidylethanolamine in assembly and function of the factor IXa-factor VIIIa complex on membrane surfaces. *Biochemistry* **39**, 13216-13222 (2000)
2. Tavoosi, N., Davis-Harrison, R. L., Pogorelov, T. V., Ohkubo, Y. Z., Arcario, M. J., Clay, M. C., Rienstra, C. M., Tajkhorshid, E., and Morrissey, J. H. Molecular determinants of phospholipid synergy in blood clotting. *The Journal of biological chemistry* **286**, 23247-23253 (2011)
3. Clark, S. R., Thomas, C. P., Hammond, V. J., Aldrovandi, M., Wilkinson, G. W., Hart, K. W., Murphy, R. C., Collins, P. W., and O'Donnell, V. B. Characterization of platelet aminophospholipid externalization reveals fatty acids as molecular determinants that regulate coagulation. *Proceedings of the National Academy of Sciences of the United States of America* **110**, 5875-5880 (2013)
4. Clark, S. R., Guy, C. J., Scurr, M. J., Taylor, P. R., Kift-Morgan, A. P., Hammond, V. J., Thomas, C. P., Coles, B., Roberts, G. W., Eberl, M., Jones, S. A., Topley, N., Kotecha, S., and O'Donnell, V. B. Esterified eicosanoids are acutely generated by 5-lipoxygenase in primary human neutrophils and in human and murine infection. *Blood* **117**, 2033-2043 (2011)
5. Hammond, V. J., Morgan, A. H., Lauder, S., Thomas, C. P., Brown, S., Freeman, B. A., Lloyd, C. M., Davies, J., Bush, A., Levonen, A. L., Kansanen, E., Villacorta, L., Chen, Y. E., Porter, N., Garcia-Diaz, Y. M., Schopfer, F. J., and O'Donnell, V. B. Novel keto-phospholipids are generated by monocytes and macrophages, detected in cystic fibrosis, and activate peroxisome proliferator-activated receptor-gamma. *The Journal of biological chemistry* **287**, 41651-41666 (2012)
6. Maskrey, B. H., Bermudez-Fajardo, A., Morgan, A. H., Stewart-Jones, E., Dioszeghy, V., Taylor, G. W., Baker, P. R., Coles, B., Coffey, M. J., Kuhn, H., and O'Donnell, V. B. Activated platelets and monocytes generate four hydroxyphosphatidylethanolamines via lipoxygenase. *The Journal of biological chemistry* **282**, 20151-20163 (2007)
7. Morgan, A. H., Dioszeghy, V., Maskrey, B. H., Thomas, C. P., Clark, S. R., Mathie, S. A., Lloyd, C. M., Kuhn, H., Topley, N., Coles, B. C., Taylor, P. R., Jones, S. A., and O'Donnell, V. B. Phosphatidylethanolamine-esterified eicosanoids in the mouse: tissue localization and inflammation-dependent formation in Th-2 disease. *The Journal of biological chemistry* **284**, 21185-21191 (2009)
8. Morgan, L. T., Thomas, C. P., Kuhn, H., and O'Donnell, V. B. Thrombin-activated human platelets acutely generate oxidized docosahexaenoic-acid-containing phospholipids via 12-lipoxygenase. *Biochem J* **431**, 141-148 (2010)
9. O'Donnell, V. B., and Murphy, R. C. New families of bioactive oxidized phospholipids generated by immune cells: identification and signaling actions. *Blood* **120**, 1985-1992 (2012)
10. Thomas, C. P., Morgan, L. T., Maskrey, B. H., Murphy, R. C., Kuhn, H., Hazen, S. L., Goodall, A. H., Hamali, H. A., Collins, P. W., and O'Donnell, V. B. Phospholipid-esterified eicosanoids are generated in agonist-activated human platelets and enhance tissue factor-dependent thrombin generation. *The Journal of biological chemistry* **285**, 6891-6903 (2010)
11. Aldrovandi, M., Hammond, V. J., Podmore, H., Hornshaw, M., Clark, S. R., Marnett, L. J., Slatter, D. A., Murphy, R. C., Collins, P. W., and O'Donnell, V. B. Human platelets generate phospholipid-esterified prostaglandins via cyclooxygenase-1 that are inhibited by low dose aspirin supplementation. *Journal of lipid research* **54**, 3085-3097 (2013)
12. Aldrovandi, M., Hinz, C., Lauder, S. N., Podmore, H., Hornshaw, M., Slatter, D. A., Tyrrell, V. J., Clark, S. R., Marnett, L. J., Collins, P. W., Murphy, R. C., and O'Donnell, V. B. DioxolaneA3-

phosphatidylethanolamines are generated by human platelets and stimulate neutrophil integrin expression. *Redox biology* **11**, 663-672 (2017)
13. Slatter, D. A., Aldrovandi, M., O'Connor, A., Allen, S. M., Brasher, C. J., Murphy, R. C., Mecklemann, S., Ravi, S., Darley-Usmar, V., and O'Donnell, V. B. Mapping the Human Platelet Lipidome Reveals Cytosolic Phospholipase A2 as a Regulator of Mitochondrial Bioenergetics during Activation. *Cell metabolism* **23**, 930-944 (2016)
14. de Groot, P. G., and Urbanus, R. T. The significance of autoantibodies against beta2-glycoprotein I. *Blood* **120**, 266-274 (2012)
15. Keeling, D., Mackie, I., Moore, G. W., Greer, I. A., Greaves, M., and British Committee for Standards in, H. Guidelines on the investigation and management of antiphospholipid syndrome. *British journal of haematology* **157**, 47-58 (2012)
16. McNally, T., Mackie, I. J., Machin, S. J., and Isenberg, D. A. Elevated levels of beta 2 glycoprotein-I (beta 2 GPI) in antiphospholipid antibody syndrome are due to increased amounts of beta 2 GPI in association with other plasma constituents. *Blood Coagul Fibrinolysis* **6**, 411-416 (1995)
17. Mann, K. G. Biochemistry and physiology of blood coagulation. *Thrombosis and haemostasis* **82**, 165-174 (1999)
18. Morrissey, J. H., Tajkhorshid, E., and Rienstra, C. M. Nanoscale studies of protein-membrane interactions in blood clotting. *Journal of thrombosis and haemostasis : JTH* **9 Suppl 1**, 162-167 (2011)
19. Zwaal, R. F., and Schroit, A. J. Pathophysiologic implications of membrane phospholipid asymmetry in blood cells. *Blood* **89**, 1121-1132 (1997)
20. Lhermusier, T., Chap, H., and Payrastre, B. Platelet membrane phospholipid asymmetry: from the characterization of a scramblase activity to the identification of an essential protein mutated in Scott syndrome. *Journal of thrombosis and haemostasis : JTH* **9**, 1883-1891 (2011)
21. Schick, P. K., Kurica, K. B., and Chacko, G. K. Location of phosphatidylethanolamine and phosphatidylserine in the human platelet plasma membrane. *The Journal of clinical investigation* **57**, 1221-1226 (1976)
22. Majumder, R., Liang, X., Quinn-Allen, M. A., Kane, W. H., and Lentz, B. R. Modulation of prothrombinase assembly and activity by phosphatidylethanolamine. *The Journal of biological chemistry* **286**, 35535-35542 (2011)
23. Huang, M., Rigby, A. C., Morelli, X., Grant, M. A., Huang, G., Furie, B., Seaton, B., and Furie, B. C. Structural basis of membrane binding by Gla domains of vitamin K-dependent proteins. *Nature structural biology* **10**, 751-756 (2003)
24. Lu, J., Pipe, S. W., Miao, H., Jacquemin, M., and Gilbert, G. E. A membrane-interactive surface on the factor VIII C1 domain cooperates with the C2 domain for cofactor function. *Blood* **117**, 3181-3189 (2011)
25. Ngo, J. C., Huang, M., Roth, D. A., Furie, B. C., and Furie, B. Crystal structure of human factor VIII: implications for the formation of the factor IXa-factor VIIIa complex. *Structure* **16**, 597-606 (2008)
26. Zwaal, R. F., Comfurius, P., and Bevers, E. M. Lipid-protein interactions in blood coagulation. *Biochimica et biophysica acta* **1376**, 433-453 (1998)
27. Palta, S., Saroa, R., and Palta, A. Overview of the coagulation system. *Indian J Anaesth* **58**, 515-523 (2014)
28. Breen, K. A., Sanchez, K., Kirkman, N., Seed, P. T., Parmar, K., Moore, G. W., and Hunt, B. J. Endothelial and platelet microparticles in patients with antiphospholipid antibodies. *Thromb Res* **135**, 368-374 (2015)
29. Chaturvedi, S., Alluri, R., and McCrae, K. R. Extracellular Vesicles in the Antiphospholipid Syndrome. *Semin Thromb Hemost* (2017)

30. Pratico, D., Ferro, D., Iuliano, L., Rokach, J., Conti, F., Valesini, G., FitzGerald, G. A., and Violi, F. Ongoing prothrombotic state in patients with antiphospholipid antibodies: a role for increased lipid peroxidation. *Blood* **93**, 3401-3407 (1999)
31. Lim, W., and Crowther, M. A. Antiphospholipid antibiodies: a critical review of the literature. *Curr Opin Hematol* **14**, 494-499 (2007)
32. Misasi, R., Capozzi, A., Longo, A., Recalchi, S., Lococo, E., Alessandri, C., Conti, F., Valesini, G., and Sorice, M. "New" antigenic targets and methodological approaches for refining laboratory diagnosis of antiphospholipid syndrome. *J Immunol Res* **2015**, 858542 (2015)
33. Lutters, B. C., Derksen, R. H., Tekelenburg, W. L., Lenting, P. J., Arnout, J., and de Groot, P. G. Dimers of beta 2-glycoprotein I increase platelet deposition to collagen via interaction with phospholipids and the apolipoprotein E receptor 2'. *The Journal of biological chemistry* **278**, 33831-33838 (2003)
34. Sikara, M. P., Routsias, J. G., Samiotaki, M., Panayotou, G., Moutsopoulos, H. M., and Vlachoyiannopoulos, P. G. {beta}2 Glycoprotein I ({beta}2GPI) binds platelet factor 4 (PF4): implications for the pathogenesis of antiphospholipid syndrome. *Blood* **115**, 713-723 (2010)
35. Vega-Ostertag, M., Harris, E. N., and Pierangeli, S. S. Intracellular events in platelet activation induced by antiphospholipid antibodies in the presence of low doses of thrombin. *Arthritis Rheum* **50**, 2911-2919 (2004)
36. Lopez-Pedrera, C., Buendia, P., Cuadrado, M. J., Siendones, E., Aguirre, M. A., Barbarroja, N., Montiel-Duarte, C., Torres, A., Khamashta, M., and Velasco, F. Antiphospholipid antibodies from patients with the antiphospholipid syndrome induce monocyte tissue factor expression through the simultaneous activation of NF-kappaB/Rel proteins via the p38 mitogen-activated protein kinase pathway, and of the MEK-1/ERK pathway. *Arthritis Rheum* **54**, 301-311 (2006)
37. Xie, H., Zhou, H., Wang, H., Chen, D., Xia, L., Wang, T., and Yan, J. Anti-beta(2)GPI/beta(2)GPI induced TF and TNF-alpha expression in monocytes involving both TLR4/MyD88 and TLR4/TRIF signaling pathways. *Mol Immunol* **53**, 246-254 (2013)
38. Sorice, M., Longo, A., Capozzi, A., Garofalo, T., Misasi, R., Alessandri, C., Conti, F., Buttari, B., Rigano, R., Ortona, E., and Valesini, G. Anti-beta2-glycoprotein I antibodies induce monocyte release of tumor necrosis factor alpha and tissue factor by signal transduction pathways involving lipid rafts. *Arthritis Rheum* **56**, 2687-2697 (2007)
39. Arvieux, J., Jacob, M. C., Roussel, B., Bensa, J. C., and Colomb, M. G. Neutrophil activation by anti-beta 2 glycoprotein I monoclonal antibodies via Fc gamma receptor II. *J Leukoc Biol* **57**, 387-394 (1995)
40. Levine, J. S., Subang, R., Koh, J. S., and Rauch, J. Induction of anti-phospholipid autoantibodies by beta2-glycoprotein I bound to apoptotic thymocytes. *J Autoimmun* **11**, 413-424 (1998)
41. Whyte, C. S., Swieringa, F., Mastenbroek, T. G., Lionikiene, A. S., Lance, M. D., van der Meijden, P. E., Heemskerk, J. W., and Mutch, N. J. Plasminogen associates with phosphatidylserine-exposing platelets and contributes to thrombus lysis under flow. *Blood* **125**, 2568-2578 (2015)
42. Yeung, J., Apopa, P. L., Vesci, J., Stolla, M., Rai, G., Simeonov, A., Jadhav, A., Fernandez-Perez, P., Maloney, D. J., Boutaud, O., Holman, T. R., and Holinstat, M. 12-lipoxygenase activity plays an important role in PAR4 and GPVI-mediated platelet reactivity. *Thrombosis and haemostasis* **110**, 569-581 (2013)
43. Yeung, J., Tourdot, B. E., Fernandez-Perez, P., Vesci, J., Ren, J., Smyrniotis, C. J., Luci, D. K., Jadhav, A., Simeonov, A., Maloney, D. J., Holman, T. R., McKenzie, S. E., and Holinstat, M. Platelet 12-LOX is essential for FcgammaRIIa-mediated platelet activation. *Blood* **124**, 2271-2279 (2014)
44. Johnson, E. N., Brass, L. F., and Funk, C. D. Increased platelet sensitivity to ADP in mice lacking platelet-type 12-lipoxygenase. *Proceedings of the National Academy of Sciences of the United States of America* **95**, 3100-3105 (1998)

45. Coates, R., Firsan SJ. Thioimidate N-oxides: nitrones of thio esters. *J Org Chem* **51**, 12 (1986)
46. Morgan, A. H., Hammond, V. J., Morgan, L., Thomas, C. P., Tallman, K. A., Garcia-Diaz, Y. R., McGuigan, C., Serpi, M., Porter, N. A., Murphy, R. C., and O'Donnell, V. B. Quantitative assays for esterified oxylipins generated by immune cells. *Nat Protoc* **5**, 1919-1931 (2010)
47. Hemker, H. C., Giesen, P. L., Ramjee, M., Wagenvoord, R., and Beguin, S. The thrombogram: monitoring thrombin generation in platelet-rich plasma. *Thrombosis and haemostasis* **83**, 589-591 (2000)
48. Horkko, S., Miller, E., Dudl, E., Reaven, P., Curtiss, L. K., Zvaifler, N. J., Terkeltaub, R., Pierangeli, S. S., Branch, D. W., Palinski, W., and Witztum, J. L. Antiphospholipid antibodies are directed against epitopes of oxidized phospholipids. Recognition of cardiolipin by monoclonal antibodies to epitopes of oxidized low density lipoprotein. *The Journal of clinical investigation* **98**, 815-825 (1996)
49. Morrow, J. D., and Minton, T. A. Improved assay for the quantification of 11-dehydrothromboxane B2 by gas chromatography-mass spectrometry. *J Chromatogr* **612**, 179-185 (1993)
50. Wang, X., and Xu, L. An optimized murine model of ferric chloride-induced arterial thrombosis for thrombosis research. *Thromb Res* **115**, 95-100 (2005)
51. *. Automated Topology Builder (ATB) and Repository. Version 2.2. Accessed on 1/7/2015*
52. Poger, D., Mark, A.E. On the Validation of Molecular Dynamics Simulations of Saturated and cis-Monounsaturated Phosphatidylcholine Lipid Bilayers: A Comparison with Experiment *J. Chem. Theory Comput* **6**, 11 (2010)
53. *. Molecular Operating environment, version 2014.09. Chemical Computing Group, Montreal, Canada*
54. *Schrödinger Release 2014-1: Desmond Molecular Dynamics System, version 3.7, D. E. Shaw Research, New York, NY, 2014. Maestro-Desmond Interoperability Tools, version 3.7, Schrödinger, New York, NY, 2014*,
55. Bowers, K., Chow, E, Xu, H, Dror, RO, Eastwood, MP, Gregersen, BA, Klepeis, JL, Kolossvary, I, Moraes, MA, Sacerdoti, FD, Salmon, JK, Shan, Y, Shaw, DE. . (2006) Scalable Algorithms for Molecular Dynamics Simulations on Commodity Clusters. in *Proceedings of the ACM/IEEE Conference on Supercomputing (SC06), Tampa, Florida,*
56. Team, R. C. (2016) R: A language and environment for statistical computing. in *R Foundation for Statistical Computing, Vienna, Austria. URL*, https://www.R-project.org/.
57. Wei, T., Simko, V. (2016) corrplot: Visualization of a Correlation Matrix. R package version 0.77. in, https://CRAN.R-project.org/package=corrplot

Acknowledgments: We thank patients and volunteers for taking part in these studies. We gratefully acknowledge assistance with tail bleeding from Dr Christopher Williams, for Nanosight experiments from Mark Gurney, for patient recruitment from Mrs Claire Nott, and technical support from Dr Christopher Rice. **Funding**: Funding is acknowledged from Wellcome Trust (094143/Z/10/Z), European Research Council (LipidArrays, VBO) and British Heart Foundation (RG/12/11/29815) (VBO, PWC), British Heart Foundation Research Fellowship (FS/11/42/28753) (CLP), the Else-Kröner Fresenius Stiftung (to GK) and The Life Sciences Research Network Wales (Welsh Computer-Aided Drug Design Platform). **Author contributions:** Experiments were conducted by SNL, DAS, GM, RU, AOC, DF, JM, SR, VJT, AB, SF, MA, MH, KAR, CPT, JA and GK, and designed by SNL, DAS, PDG, SH, VBO, SAJ, PRT, PWC, PVJ. CLP and SO provided clinical samples. AP provided supervision and training. SNL, DAS, VBO and PWC wrote the paper. All authors edited the manuscript. **Competing interests:** The authors have declared that they have no competing interests.

Fig. 1. HETE-PEs and HETE-PCs dose-dependently enhance TF-dependent thrombin generation through a PS-dependent mechanism. Thrombin generation was initiated by the addition of liposomes to pooled platelet-poor plasma (PPP) with a thrombinoscope as described in Materials and Methods. (**A**) HETE-PEs enhance TF-dependent thrombin generation in plasma. Liposomes contained 10 pM recombinant TF with 65 % DSPC, 5 % SAPS, and 30 % SAPE, with 0 to 10 % SAPE replaced with 0 to 10 % of the indicated HETE-PE species. (**B**). HETE-PCs enhance TF-dependent thrombin generation in plasma. Liposomes contained 10 pM TF, 55 % DSPC, 5 % SAPS, 30 % SAPE, with 0 to 10 % SAPC replaced with < 10 % of the indicated HETE-PC species. Data in (A) and (B) are representative traces of experiments that were repeated at least 3 times. (**C**) 15-HETE-PE and 15-HETE-PC enhance PS-dependent thrombin generation. Pooled PPP was activated with liposomes as described earlier, where SAPE was replaced with 15-HETE-PE (left graphs) or 15-HETE-PC (right graphs), with or without SAPS replacing PC, as indicated. Representative traces and maximum thrombin at varying PS concentrations are shown. Data are means ± SEM of three runs. (**D**) HETE-PE and HETE-PCs promote the activities of coagulation factors in a full reconstitution system. Thrombin generation was initiated by the addition of liposomes to purified factors II, V, VII, VIIII, IX, X at physiological concentrations (see Materials and Methods). Liposomes contained (left) 65 % DSPC, 5 % SAPS, 30 % SAPE, with 10 % SAPE (control) or 10 % HETE-PE or (middle) 55 % DSPC, 5 % SAPS, 30 % SAPE, 10 % SAPC (control) or 10% HETE-PC. Right: Summary data presented as fold-change for the maximum thrombin generation rate observed (slope of lines in left and middle graphs) for each isomer. Data are means ± SEM of three runs. *$p < 0.05$, **$p < 0.01$ by single-factor ANOVA and post-hoc Tukey tests.

Fig. 2. MD simulation suggests the association of the HETE-PL hydroxyl group with the polar environment, serine, and Ca^{2+}, whereas HETE-PL membranes bind more Ca^{2+}. (**A** to **E**) MD

simulation shows the HETE hydroxyl group altering membrane behavior. MD simulations were undertaken for 300 ns using 5% SAPS, 5% SAPC, 30% SAPE, 55% DOPC, 5% 12-HETE-PC as described in Materials Methods. (A to D) Side views showing hydrophobic (yellow), charged phosphate groups (cyan), and PC headgroups (grey). (E) Top view looking down on the membrane showing areas of positive charge (blue), negative charge (brown), PS headgroups (pink), and HETE hydroxyl groups (red). (**F**) Binding of calcium to membranes is increased by 15-HETE-PE. Liposomes consisting of 65 % DSPC, 30 % SAPE, and 5 % SAPS, with up to 10 % SAPE replaced by 15-HETE PE were tested for calcium binding by measuring Fluo-FF fluorescence (see Materials and Methods). *p<0.05, **p<0.01 when compared to no added 15-HETE-PE. Data are means ± SEM of three experiments and were analyzed with the Mann Whitney U test.

Fig. 3. HETE-PL liposomes prevent tail bleeding and increase TAT concentrations in vivo, whereas platelets from mice genetically lacking p12-LOX generate few eoxPLs. (**A**) 12-HETE-PE/TF intradermal administration prevents tail bleeding in adult mice. 11-week old male C57BL/6J mice were injected with liposomes containing TF with or without 12-HETE-PE or 12-HETE-PC immediately proximal of a tail cut and bleeding time and blood loss were recorded as described in Materials and Methods. Data are from 10 to 16 mice per group. ** $p \leq 0.01$, * $p \leq 0.05$ by Mann Whitney U test. (**B**) 12-HETE-PE increases thrombin-anti-thrombin (TAT) complexes in vivo. Control or HETE-PE-containing liposomes were injected i.v. into wild-type mice and plasma was obtained after 1 hr. TAT concentrations were measured by ELISA. Data are from 6 mice per group. * $p \leq 0.05$). (**C**) Thrombin stimulates the production of eoxPL species from washed murine platelets in a p12-LOX–dependent manner. Washed platelets from wild-type or *ALOX12*$^{-/-}$ mice were activated for 30 min with 0.2 U/ml thrombin and then the lipids extracted and analyzed to detect eoxPL species. Data are means of three experiments. Data in the heatmap are normalized to basal amounts of the indicated eoxPLs in wild-type mouse platelets. (**D**) Time course for the generation

of 12-HETE-PE and 12-HETE–PCs. Platelets from wild-type or *ALOX12* $^{-/-}$ mice (2 x 10^8/ml) were activated with 0.2 U/ml human thrombin for 0 to 30 min at 37 °C. The lipids wer then extracted and quantified. HETE-PE represents the sum of 16:0p/12-HETE-PE, 18:1p/12-HETE-PE, 18:0/12-HETE-PE, and 18:0a/HETE PE. HETE-PC represents the sum of 16:0a/12-HETE-PC and 18:0a/12-HETE-PC. Data are means ± SEM of 8 mice per group.

Fig. 4. Mice lacking either 12/15-LOX or p12-LOX have impaired venous coagulation, which is restored by the administration of 12-HETE-PE liposomes. (**A** and **B**) *ALOX12*-deficient mice show reduced thrombus formation in vivo after challenge. Venous thrombosis was induced in WT and ALOX12$^{-/-}$ mice. (A) Thrombus weights were measured. Data area means + SEM of 7 to 9 mice per group, * $p<0.05$ by Mann Whitney U test). (B) A representative thrombus is shown for each genotype. (C) ALOX12–deficient mice have impaired hemostasis in vivo. 8-11 week old male wild-type C57BL/6J or ALOX12$^{-/-}$ mice were administered a tail cut, and bleeding time and blood loss were recorded. Liposomes containing 19 ng 12-HETE-PE or control liposomes were administered in 10 ml PBS, into the tail tissue, just ahead of the cut, and immediately before the cut was made. Data are means + SEM of 6 to 12 mice per group. (D) ALOX12- and ALOX15-–deficient mice have impaired hemostasis in vivo. Experiments were performed and data were collected as described in (C) except that wild-type C57BL/6J mice were compared to ALOX12- and ALOX15-deficient mice. Data are means + SEM of 12 to 19 mice per group. Data in (C) and (D) were analyzed by Mann Whitney U test, * $p< 0.05$, ** $p < 0.01$, *** $p< 0.005$).

Fig. 5. HETE-PEs are increased in leukocytes and platelets from APS patients. (**A** and **B**) 15- and 5-HETE-PEs are increased in leukocytes from APS patients. Total leukocytes were isolated from HCs and APS patients, left unstimulated (US) or stimulated at 4 x 10^6 cells/ml with 10 μM A23187 for 30 min at 37 °C, and then the lipids were analyzed for HETE-PEs. HETE-PEs were

quantified as individual molecular species and then were combined. Data area means + SEM of 34 (HC) or 17 (APS) subjects. (**C**) 12-HETE-PEs are increased in platelets from APS patients. Washed platelets from HCs and APS patients were isolated and left unstimulated or stimulated with 0.2 U/ml thrombin for 30 min at 37 °C before the amounts of 12-HETE-PE were determined. Data are means + SEM of 18 (HC) or 12 (APS) subjects. (**D**) Platelets from APS patients that spontaneously aggregated contain substantial amounts of 12-HETE-PEs. During the final washing step, a number of APS platelet isolates spontaneously aggregated (n = 7 patients). Lipids were extracted and analyzed for 12-HETE-PEs. (**E**) Urinary TXB_2 is increased in APS patients. Urine from HCs and APS patients was analyzed by GC/MS to determine the amounts of TXB2. Data are means + SEM of 32 (HC) or 9 (APS) subjects. (**F** and **G**) 15- and 5-HETE-PEs are basally increased in concentration in platelets from APS patients. Platelets were prepared as described in (C) and then were analyzed to determine the amounts of the indicated HETE-PEs. Data are means + SEM of 18 (HC) or 12 (APS) subjects. (**H**) 12-HETE-PEs are basally increased in abundance in leukocytes from APS patients. Total leukocytes were isolated and left unstimulated or stimulated at 4 x 10^6 cells/ml with 10 mm A23187 for 30 min at 37°C and then analyzed for 12-HETE-PEs. Data area means + 34 (HC) or 18 (APS) subjects. *** $p \leq 0.001$, ** $p \leq 0.01$, * $p \leq 0.05$ by Mann Whitney U test.

Fig. 6. Circulating IgG against HETE-PEs is increased in abundance in APS and β2BP1 binding to membranes is enhanced by HETE-PEs. (**A** to **C**) IgG against HETE-PEs are statistically significantly increased in abundance in plasma from APS patients. The amounts of IgG antibodies against HETE-PEs in HC and APS patient plasma were determined by diluting plasma 1:12 and testing binding to the indicated antigens. SAPE was used as an unoxidized lipid for comparison. All samples were analyzed in triplicate. Data are means + SEM of 18 (HC) or 9 (APS) subjects. * $p < 0.05$, ** p 0.01 by Mann Whitney U test. (**D**) IgG titers are comparable in plasma

from HCs and APS patients. Total IgG amounts in plasma from HCs and APS patients were determined. Data are means + SEM of 34 (HC) and 10 (APS) subjects. (**E**) HETE-PEs enhance the binding of β2GPI to lipid membranes. Binding of β2GPI to liposomes in the presence of cardiolipin, 15-HETE-PE, 5-HETE-PE, or 12-HETE-PE was determined as described in Materials and Methods. (F) HETE-PEs enhance the cardiolipin-dependent binding of β2GPI to lipids. Binding of β2GPI to liposomes in the presence of cardiolipin with or without 15-HETE-PE, 5-HETE-PE or 12-HETE-PE was determined. In (D) and (E) data are means ± SEM of three experiments each performed in triplicate. Statistical significance was determined by one-way ANOVA and Tukey-Kramers test. * $p < 0.05$, ** p 0.01, *** $P < 0.001$.

Fig. 7. Lipidomic profiling of 47 eoxPL defines their enzymatic origin and regulatory networks. (**A** and **B**) Washed platelets were isolated from HCs or APS patients and were left unstimulated or were stimulated with thrombin (0.2 U/ml, 30 min) before lipids were extracted and analyzed by LC/MS/MS for 47 eoxPL species as described in Materials and Methods. Data are from 16 (HC) and 10 (APS) subjects. (A) p12-LOX– and COX-1–derived lipids cluster into distinct families based on Sn2 fatty acid composition. A heatmap of the effect of thrombin on the abundances of the indicated lipids is shown. In the heatmap, an increase in abundance is denoted in red, whereas a decrease in abundance is denoted in blue. Deeper tones indicate greater differences, with comparisons for individual lipids made across samples. (B) Plotting correlation between individual lipids illustrates additional relatedness between families of ions. Correlations between lipids across the whole cohort were plotted in a grid in order of decreasing correlation with 18:0a/12-HETE-PE (see fig. S4 and Materials and Methods). Red: p12-LOX, blue: COX-1, green: polyoxygenated PL, black: unknown origin. Lipids marked with red arrows indicating a relationship are listed. All lipid abundances were normalized to the mean of those of the control unstimulated values.

Fig. 8. Cytoscape network confirms the enzymatic origin of lipids and identifies an additional group regulated independently of known pathways; p12-LOX–derived eoxPLs are statisitically significantly increased in APS patient platelets. (**A**) A Cytoscape network correlation identifies three groups of eoxPLs. Cytoscape 1.2.3 correlation was performed (correlation > 0.8) using data shown in Fig. 7A, with nodes as individual lipids and size determined by the number of links to others. Edge thickness represents the extent of the correlation between individual nodes. Lipids were identified as COX-1– or p12-LOX–derived based on aspirin sensitivity or their absence in *ALOX12*$^{-/-}$ mice. The plasmalogen-PE group was not associated with any enzymatic system. All lipid abundances were normalized to the mean of the control unstimulated values. (**B**) p12-LOX–derived lipids are statistically significantly increased in abundance in platelets from patients with APS. Platelet lipids identified as originating from p12-LOX (n = 31) or COX-1 (n = 9) as determined with the Cytoscape network were examined as separate groups for statistically significant differences using the Mann-Whitney U test. * $p < 0.05$, ** p 0.01, *** P <0.001.

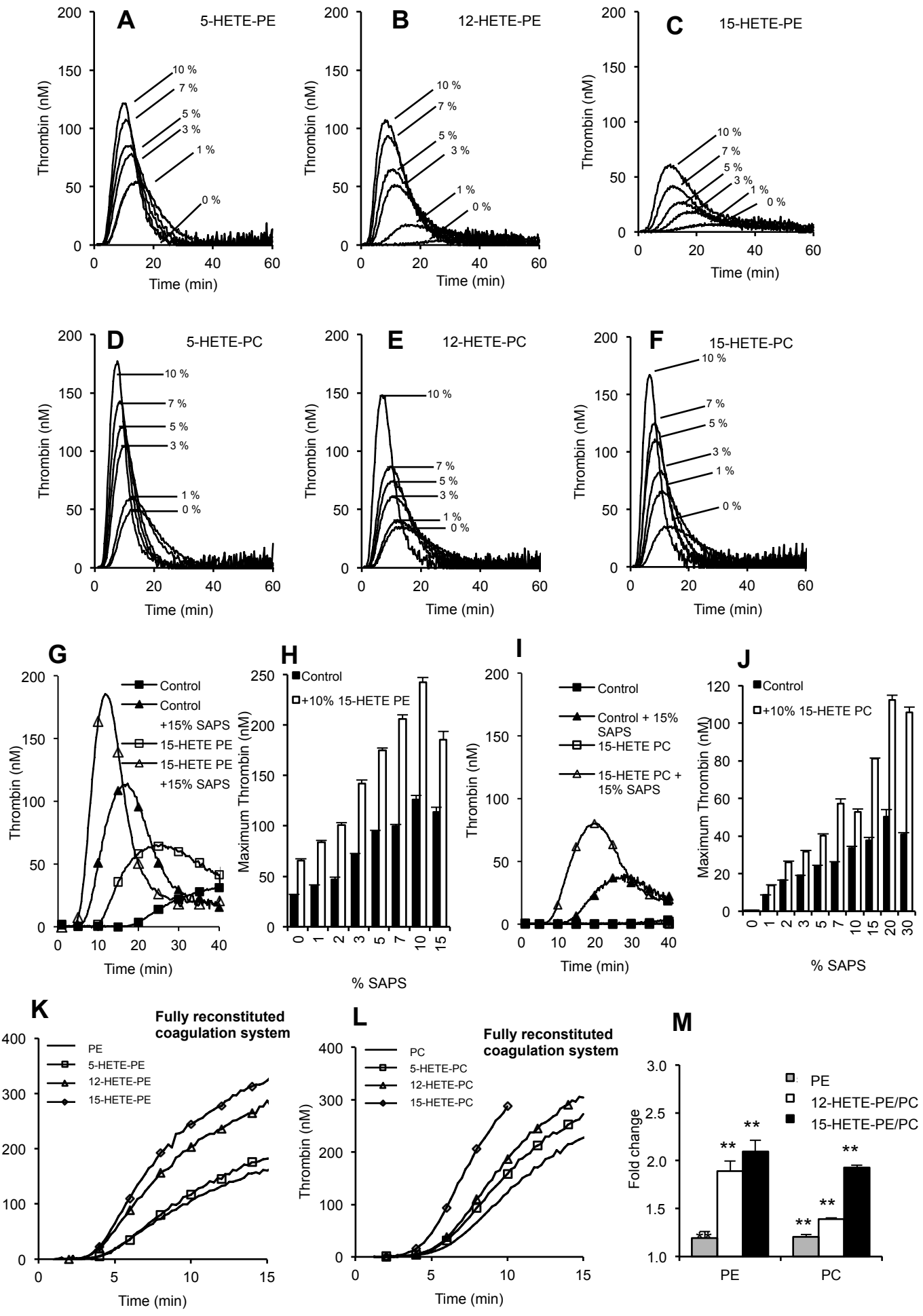
A
5-HETE-PE
B
12-HETE-PE
C
15-HETE-PE
D
5-HETE-PC
E
12-HETE-PC
F
15-HETE-PC
Thrombin (nM)
Time (min)
10 %
7 %
5 %
3 %
1 %
0 %
G
Control
Control +15% SAPS
15-HETE PE
15-HETE PE +15% SAPS
H
Control
+10% 15-HETE PE
Maximum Thrombin (nM)
% SAPS
I
Control
Control + 15% SAPS
15-HETE PC
15-HETE PC + 15% SAPS
J
Control
+10% 15-HETE PC
K
Fully reconstituted coagulation system
PE
5-HETE-PE
12-HETE-PE
15-HETE-PE
L
Fully reconstituted coagulation system
PC
5-HETE-PC
12-HETE-PC
15-HETE-PC
M
PE
12-HETE-PE/PC
15-HETE-PE/PC
Fold change
**
PE
PC

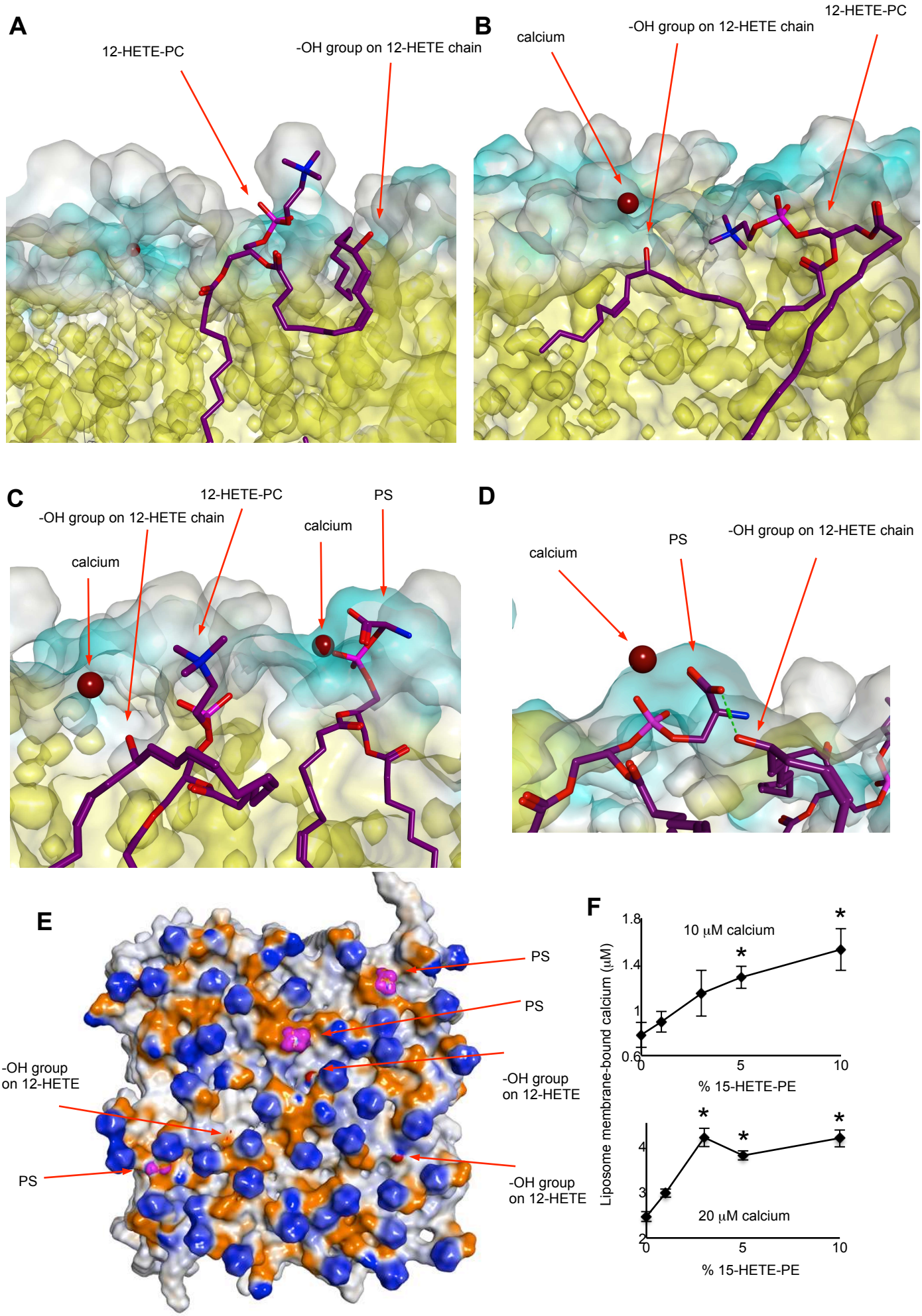
A
12-HETE-PC
-OH group on 12-HETE chain
B
calcium
-OH group on 12-HETE chain
12-HETE-PC
C
-OH group on 12-HETE chain
12-HETE-PC
PS
calcium
calcium
D
calcium
PS
-OH group on 12-HETE chain
E
PS
PS
-OH group on 12-HETE
-OH group on 12-HETE
PS
-OH group on 12-HETE
F
10 μM calcium
Liposome membrane-bound calcium (μM)
1.8
1.4
1
0.6
0
5
10
% 15-HETE-PE
20 μM calcium
4
3
2
0
5
10
% 15-HETE-PE

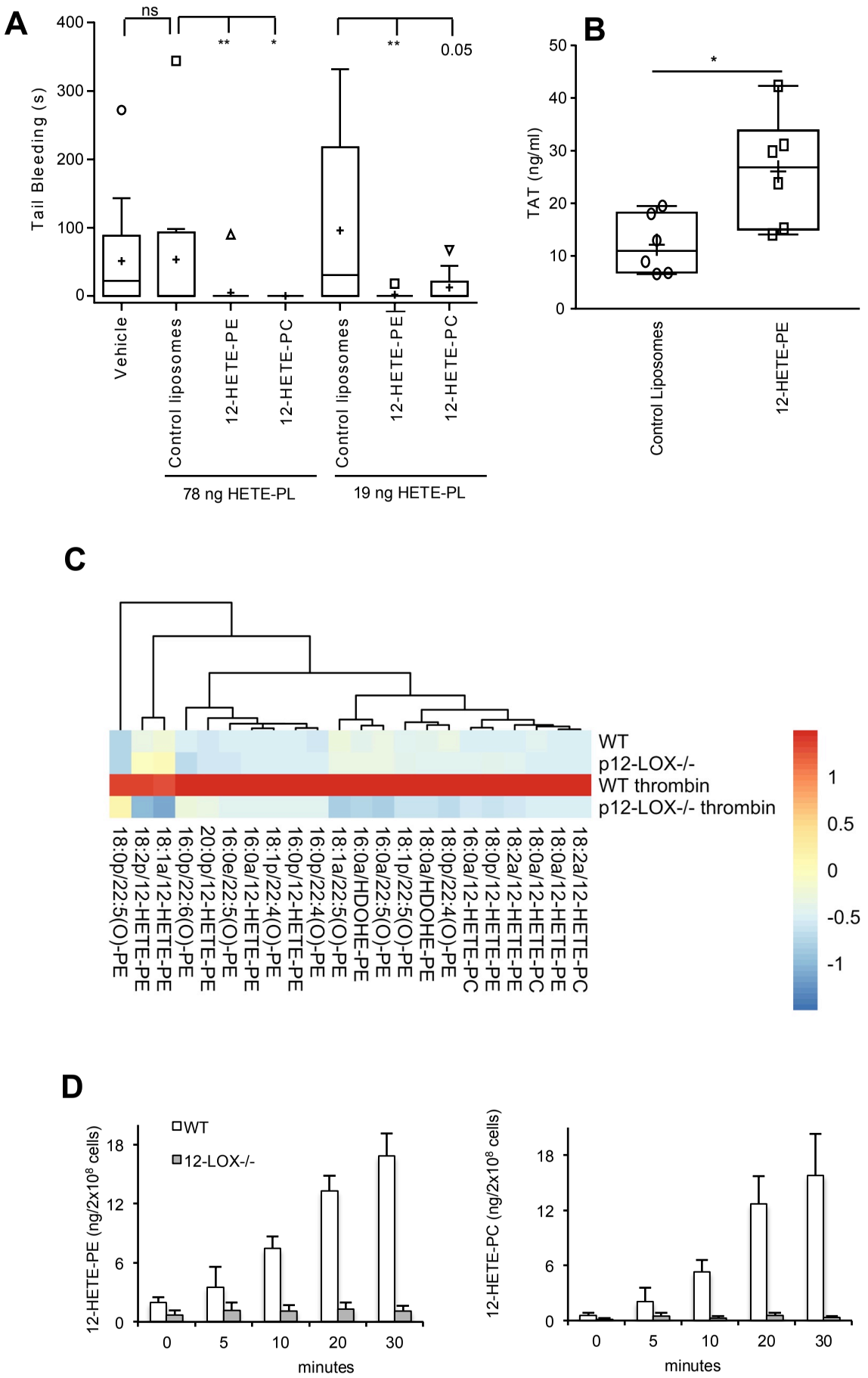
A
Tail Bleeding (s)
400
300
200
100
0
ns
**
*
**
0.05
Vehicle
Control liposomes
12-HETE-PE
12-HETE-PC
Control liposomes
12-HETE-PE
12-HETE-PC
78 ng HETE-PL
19 ng HETE-PL
B
TAT (ng/ml)
50
40
30
20
10
0
*
Control Liposomes
12-HETE-PE
C
WT
p12-LOX-/-
WT thrombin
p12-LOX-/- thrombin
1
0.5
0
-0.5
-1
18:0p/22:5(O)-PE
18:2p/12-HETE-PE
18:1a/12-HETE-PE
16:0p/22:6(O)-PE
20:0p/12-HETE-PE
16:0e/22:5(O)-PE
16:0a/12-HETE-PE
18:1p/22:4(O)-PE
16:0p/12-HETE-PE
16:0p/22:4(O)-PE
18:1a/22:5(O)-PE
16:0a/HDOHE-PE
16:0a/22:5(O)-PE
18:1p/22:5(O)-PE
18:0a/HDOHE-PE
18:0p/22:4(O)-PE
16:0a/12-HETE-PC
18:0p/12-HETE-PE
18:2a/12-HETE-PE
18:0a/12-HETE-PC
18:0a/12-HETE-PE
18:2a/12-HETE-PC
D
12-HETE-PE (ng/2x10^8 cells)
WT
12-LOX-/-
18
12
6
0
0
5
10
20
30
minutes
12-HETE-PC (ng/2x10^8 cells)
18
12
6
0
0
5
10
20
30
minutes

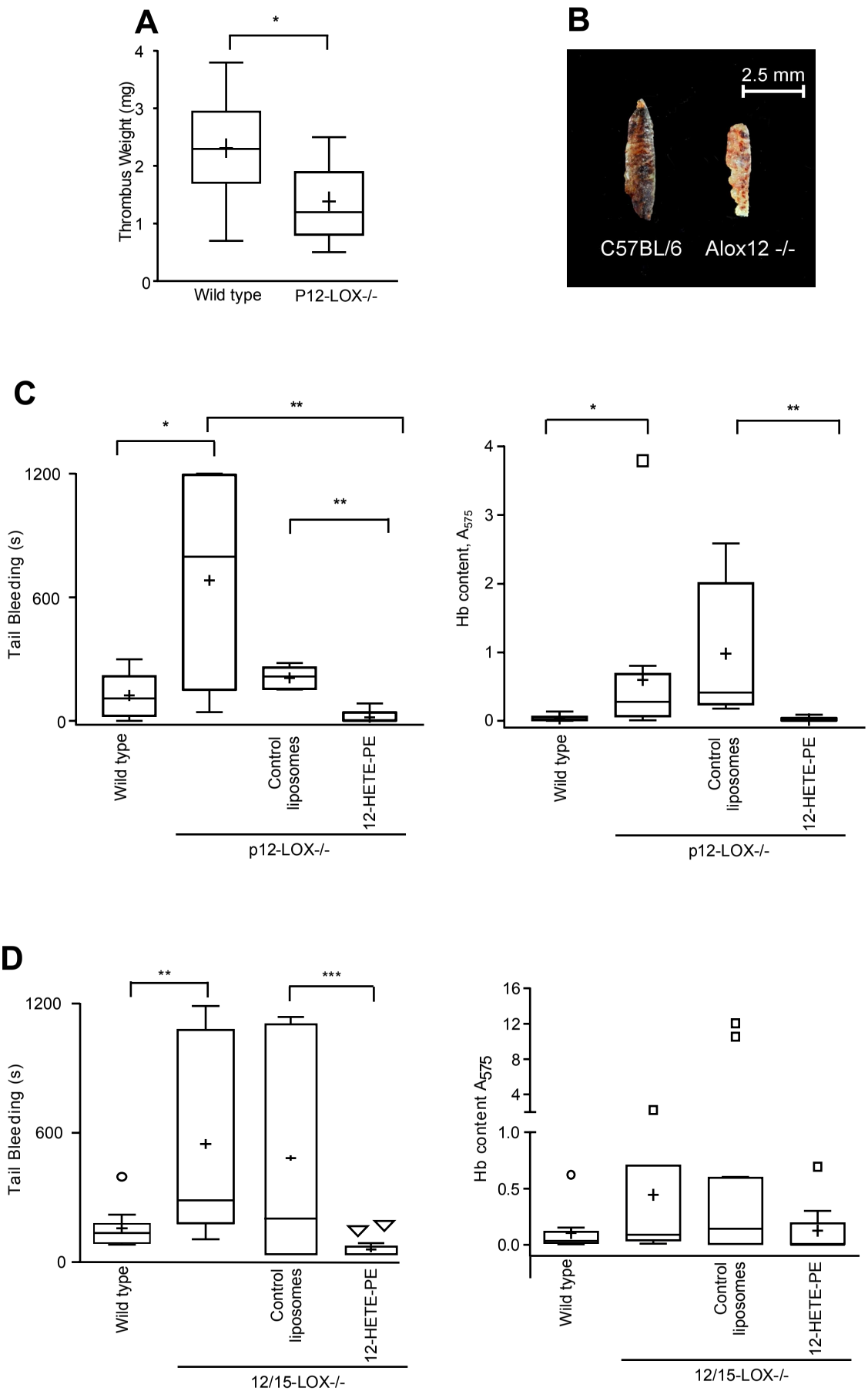
A
*
Thrombus Weight (mg)
4
3
2
1
0
Wild type
P12-LOX-/-
B
2.5 mm
C57BL/6
Alox12 -/-
C
*
**
Tail Bleeding (s)
1200
600
0
**
Wild type
Control liposomes
12-HETE-PE
p12-LOX-/-
*
**
Hb content, A575
4
3
2
1
0
Wild type
Control liposomes
12-HETE-PE
p12-LOX-/-
D
**
***
Tail Bleeding (s)
1200
600
0
Wild type
Control liposomes
12-HETE-PE
12/15-LOX-/-
Hb content A575
16
12
8
4
1.0
0.5
0.0
Wild type
Control liposomes
12-HETE-PE
12/15-LOX-/-

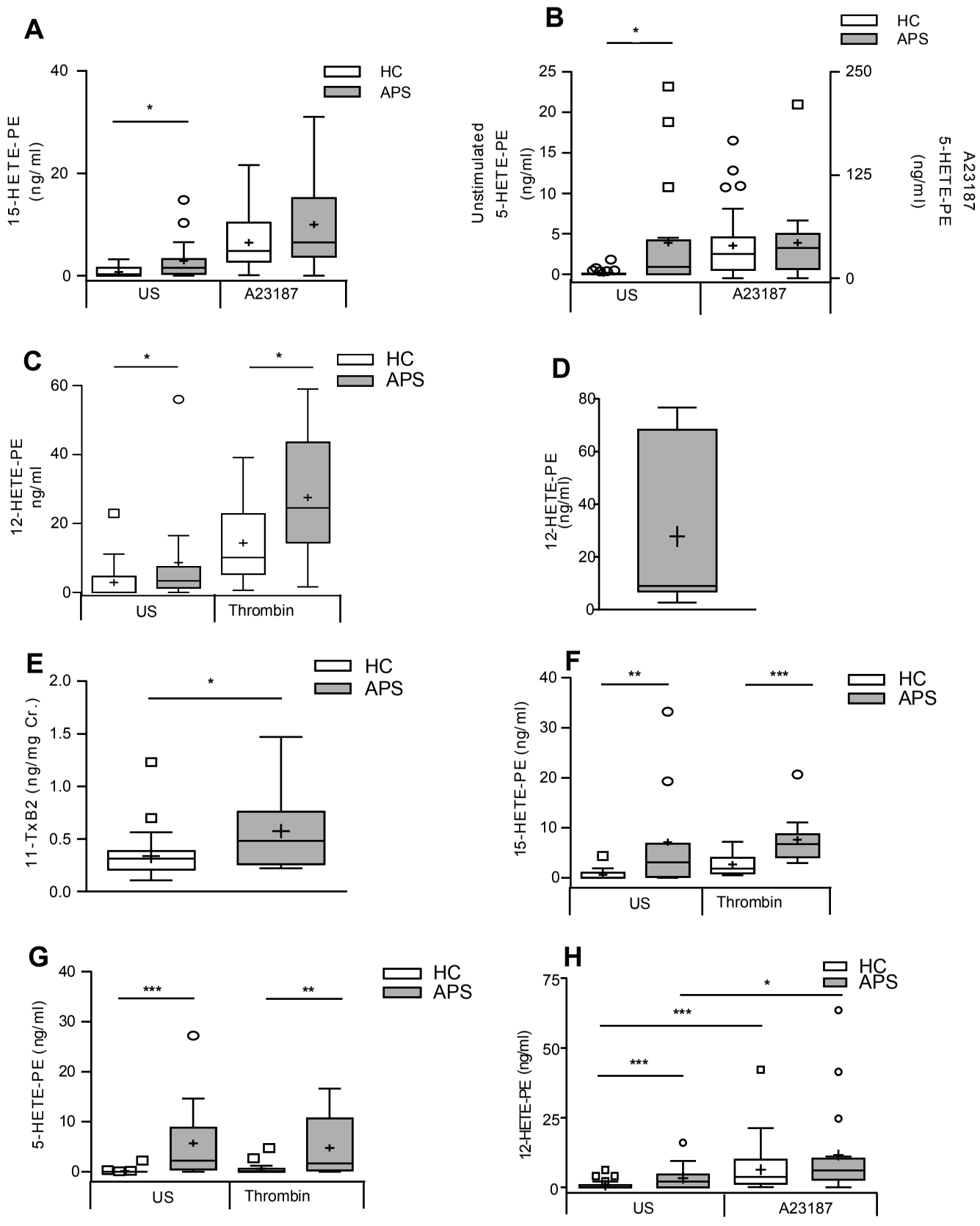
A
15-HETE-PE (ng/ml)
HC
APS
US
A23187
B
Unstimulated 5-HETE-PE (ng/ml)
A23187 5-HETE-PE (ng/ml)
C
12-HETE-PE ng/ml
Thrombin
D
12-HETE-PE (ng/ml)
E
11-TxB2 (ng/mg Cr.)
F
15-HETE-PE (ng/ml)
G
5-HETE-PE (ng/ml)
H
12-HETE-PE (ng/ml)

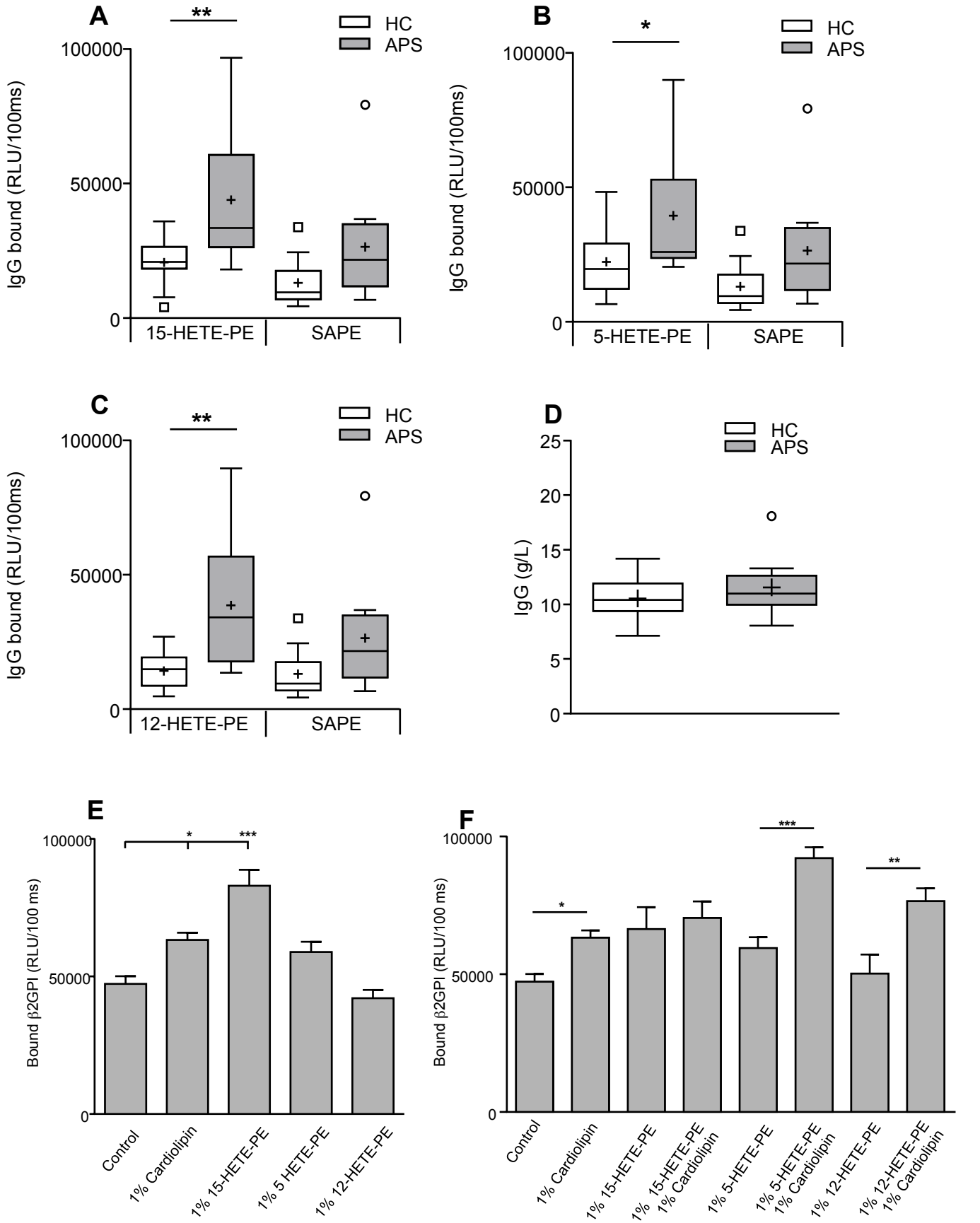
A
**
HC
APS
IgG bound (RLU/100ms)
100000
50000
0
15-HETE-PE
SAPE
B
*
HC
APS
IgG bound (RLU/100ms)
100000
50000
0
5-HETE-PE
SAPE
C
**
HC
APS
IgG bound (RLU/100ms)
100000
50000
0
12-HETE-PE
SAPE
D
HC
APS
IgG (g/L)
25
20
15
10
5
0
E
*
***
Bound β2GPI (RLU/100 ms)
100000
50000
0
Control
1% Cardiolipin
1% 15-HETE-PE
1% 5 HETE-PE
1% 12-HETE-PE
F
*
***
**
Bound β2GPI (RLU/100 ms)
100000
50000
0
Control
1% Cardiolipin
1% 15-HETE-PE
1% 15-HETE-PE 1% Cardiolipin
1% 5-HETE-PE
1% 5-HETE-PE 1% Cardiolipin
1% 12-HETE-PE
1% 12-HETE-PE 1% Cardiolipin

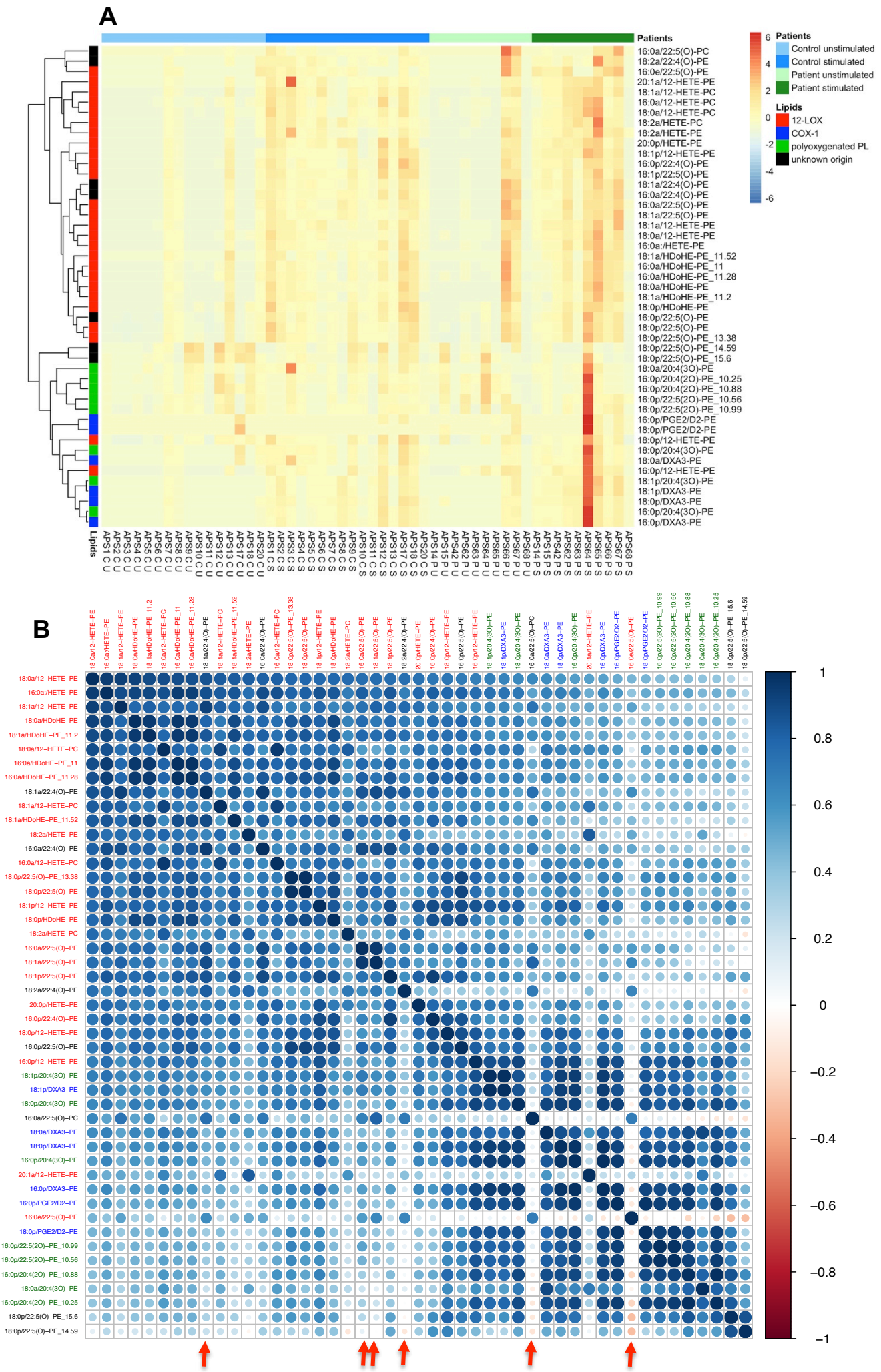
A
Patients
Control unstimulated
Control stimulated
Patient unstimulated
Patient stimulated
Lipids
12-LOX
COX-1
polyoxygenated PL
unknown origin
6
4
2
0
-2
-4
-6
16:0a/22:5(O)-PC
18:2a/22:4(O)-PE
16:0e/22:5(O)-PE
20:1a/12-HETE-PE
18:1a/12-HETE-PC
16:0a/12-HETE-PC
18:0a/12-HETE-PC
18:2a/HETE-PC
18:2a/HETE-PE
20:0p/HETE-PE
18:1p/12-HETE-PE
16:0p/22:4(O)-PE
18:1p/22:5(O)-PE
18:1a/22:4(O)-PE
16:0a/22:4(O)-PE
16:0a/22:5(O)-PE
18:1a/22:5(O)-PE
18:1a/12-HETE-PE
18:0a/12-HETE-PE
16:0a/HETE-PE
18:1a/HDoHE-PE_11.52
16:0a/HDoHE-PE_11
16:0a/HDoHE-PE_11.28
18:0a/HDoHE-PE
18:1a/HDoHE-PE_11.2
18:0p/HDoHE-PE
16:0p/22:5(O)-PE
18:0p/22:5(O)-PE
18:0p/22:5(O)-PE_13.38
18:0p/22:5(O)-PE_14.59
18:0p/22:5(O)-PE_15.6
18:0a/20:4(3O)-PE
16:0p/20:4(2O)-PE_10.25
16:0p/20:4(2O)-PE_10.88
16:0p/22:5(2O)-PE_10.56
16:0p/22:5(2O)-PE_10.99
16:0p/PGE2/D2-PE
18:0p/PGE2/D2-PE
18:0p/12-HETE-PE
18:0p/20:4(3O)-PE
18:0a/DXA3-PE
16:0p/12-HETE-PE
18:1p/20:4(3O)-PE
18:1p/DXA3-PE
18:0p/DXA3-PE
16:0p/20:4(3O)-PE
16:0p/DXA3-PE
Lipids
APS1 C U
APS2 C U
APS3 C U
APS4 C U
APS5 C U
APS6 C U
APS7 C U
APS8 C U
APS9 C U
APS10 C U
APS11 C U
APS12 C U
APS13 C U
APS17 C U
APS18 C U
APS20 C U
APS1 C S
APS2 C S
APS3 C S
APS4 C S
APS5 C S
APS6 C S
APS7 C S
APS8 C S
APS9 C S
APS10 C S
APS11 C S
APS12 C S
APS13 C S
APS17 C S
APS18 C S
APS20 C S
APS15 P U
APS42 P U
APS62 P U
APS63 P U
APS64 P U
APS65 P U
APS66 P U
APS67 P U
APS68 P U
APS14 P S
APS15 P S
APS42 P S
APS62 P S
APS63 P S
APS64 P S
APS65 P S
APS66 P S
APS67 P S
APS68 P S
B
18:0a/12-HETE-PE
16:0a/HETE-PE
18:1a/12-HETE-PE
18:0a/HDoHE-PE
18:1a/HDoHE-PE_11.2
18:0a/12-HETE-PC
16:0a/HDoHE-PE_11
16:0a/HDoHE-PE_11.28
18:1a/22:4(O)-PE
18:1a/12-HETE-PC
18:1a/HDoHE-PE_11.52
18:2a/HETE-PE
16:0a/22:4(O)-PE
16:0a/12-HETE-PC
18:0p/22:5(O)-PE_13.38
18:0p/22:5(O)-PE
18:1p/12-HETE-PE
18:0p/HDoHE-PE
18:2a/HETE-PC
16:0a/22:5(O)-PE
18:1a/22:5(O)-PE
18:1p/22:5(O)-PE
18:2a/22:4(O)-PE
20:0p/HETE-PE
16:0p/22:4(O)-PE
18:0p/12-HETE-PE
16:0p/22:5(O)-PE
16:0p/12-HETE-PE
18:1p/20:4(3O)-PE
18:1p/DXA3-PE
18:0p/20:4(3O)-PE
16:0a/22:5(O)-PC
18:0a/DXA3-PE
18:0p/DXA3-PE
16:0p/20:4(3O)-PE
20:1a/12-HETE-PE
16:0p/DXA3-PE
16:0p/PGE2/D2-PE
16:0e/22:5(O)-PE
18:0p/PGE2/D2-PE
16:0p/22:5(2O)-PE_10.99
16:0p/22:5(2O)-PE_10.56
16:0p/20:4(2O)-PE_10.88
18:0a/20:4(3O)-PE
16:0p/20:4(2O)-PE_10.25
18:0p/22:5(O)-PE_15.6
18:0p/22:5(O)-PE_14.59
1
0.8
0.6
0.4
0.2
0
−0.2
−0.4
−0.6
−0.8
−1

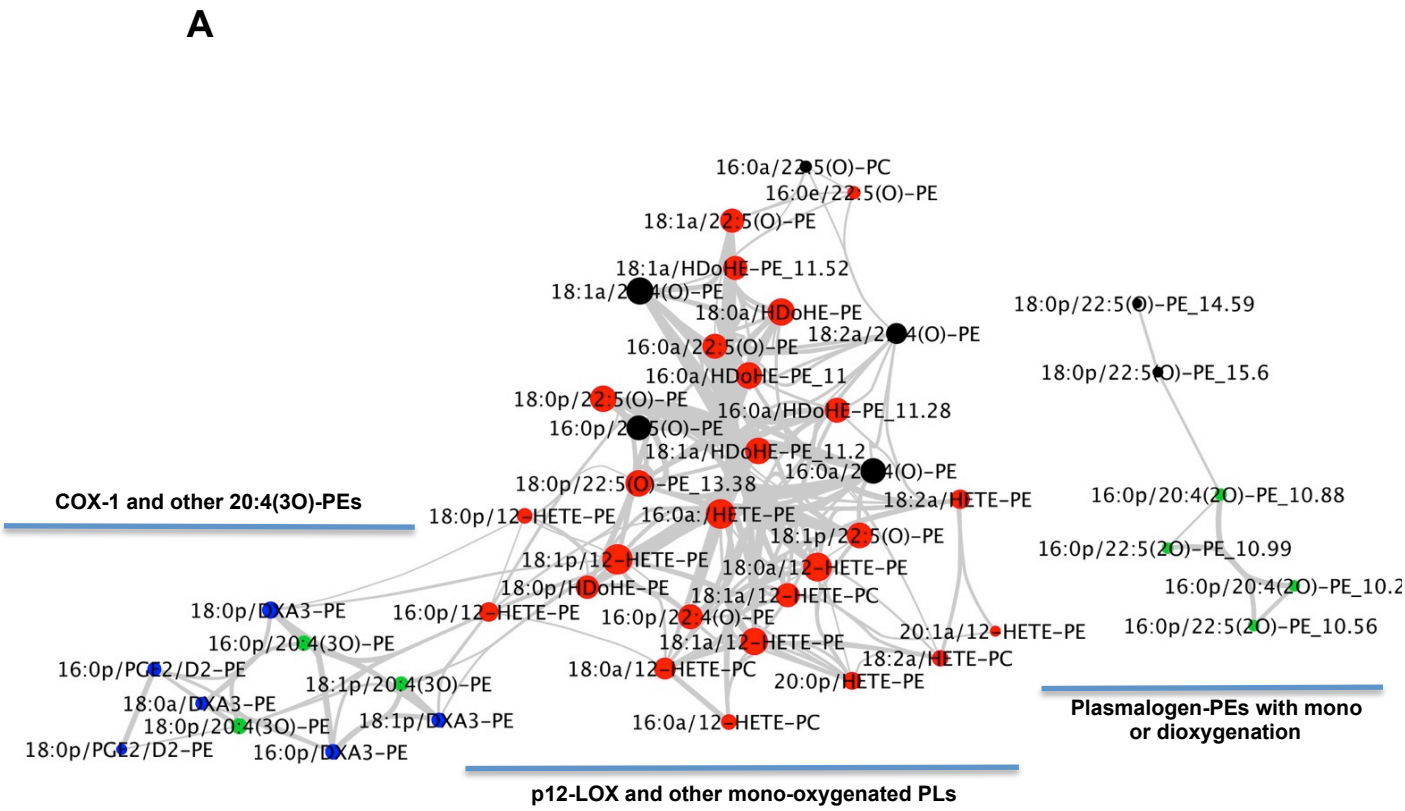
A
16:0a/22:5(O)-PC
16:0e/22:5(O)-PE
18:1a/20:5(O)-PE
18:1a/HDoHE-PE_11.52
18:1a/20:4(O)-PE
18:0a/HDoHE-PE
18:2a/20:4(O)-PE
16:0a/22:5(O)-PE
16:0a/HDoHE-PE_11
18:0p/22:5(O)-PE
16:0a/HDoHE-PE_11.28
16:0p/20:5(O)-PE
18:1a/HDoHE-PE_11.2
16:0a/20:4(O)-PE
18:0p/22:5(O)-PE_13.38
18:2a/HETE-PE
18:0p/12-HETE-PE
16:0a/HETE-PE
18:1p/22:5(O)-PE
18:1p/12-HETE-PE
18:0a/12-HETE-PE
18:0p/HDoHE-PE
18:1a/12-HETE-PC
18:0p/DXA3-PE
16:0p/12-HETE-PE
16:0p/22:4(O)-PE
16:0p/20:4(3O)-PE
18:1a/12-HETE-PE
20:1a/12-HETE-PE
16:0p/PC22/D2-PE
18:2a/HETE-PC
18:1p/20:4(3O)-PE
18:0a/12-HETE-PC
20:0p/HETE-PE
18:0a/DXA3-PE
18:0p/20:4(3O)-PE
18:1p/DXA3-PE
16:0a/12-HETE-PC
18:0p/PC22/D2-PE
16:0p/DXA3-PE
COX-1 and other 20:4(3O)-PEs
p12-LOX and other mono-oxygenated PLs
18:0p/22:5(O)-PE_14.59
18:0p/22:5(O)-PE_15.6
16:0p/20:4(2O)-PE_10.88
16:0p/22:5(2O)-PE_10.99
16:0p/20:4(2O)-PE_10.2
16:0p/22:5(2O)-PE_10.56
Plasmalogen-PEs with mono or dioxygenation

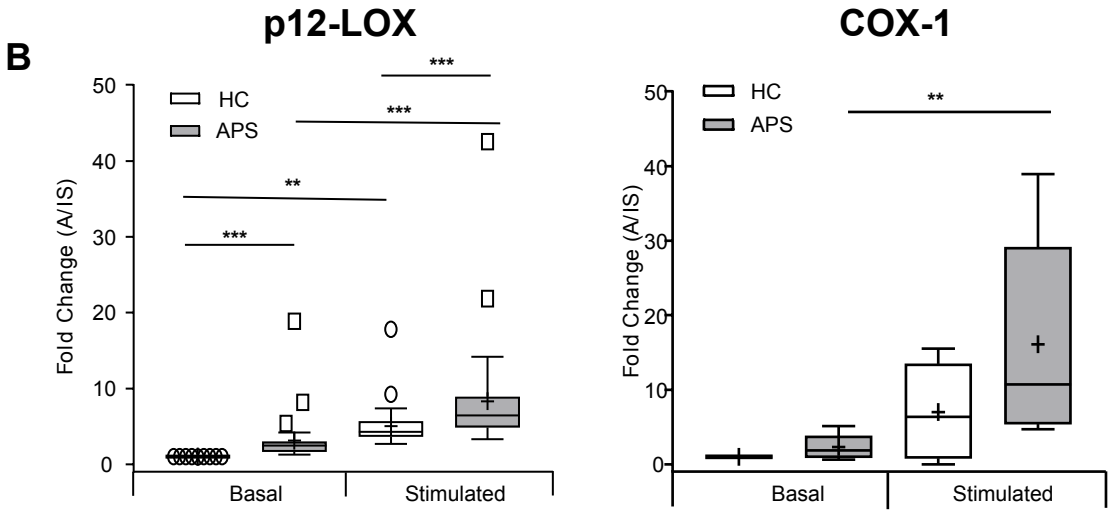
B
p12-LOX
COX-1
HC
APS
Fold Change (A/IS)
0
10
20
30
40
50
Basal
Stimulated
***
**